Perception of Temperature Even in the Absence of Actual Change is Sufficient to Drive Transgenerational Epigenetic Inheritance

Guy Teichman[1*#], Mor Sela[1#], Chee Kiang Ewe[1#], Itai Rieger[1], Sarit Anava[1], Yael Mor[1], Péter Szántó[2,3], David H. Meyer[2,3], Hila Doron[1], Or Shachar[4], Vladyslava Pechuk[5], Hila Gingold[1], Meital Oren-Suissa[5], Matthew McGee[6], Michael Shapira[6], Björn Schumacher[2,3], Oded Rechavi[1*]

[1]School of Neurobiology, Biochemistry and Biophysics, Wise Faculty of Life Sciences & Sagol School of Neuroscience, Tel Aviv University, Tel Aviv, Israel.

[2]Institute for Genome Stability in Aging and Disease, Medical Faculty, University of Cologne, Germany

[3]Cologne Excellence Cluster for Cellular Stress Responses in Ageing-Associated Diseases (CECAD), Center for Molecular Medicine Cologne (CMMC), University of Cologne, Joseph-Stelzmann-Str. 26, 50931 Cologne, Germany

[4]Migal Galilee Research Institute, Kiryat Shmona, Israel

[5]Department of Brain Sciences, Faculty of Biology, Weizmann Institute of Science, Rehovot, Israel

[6]Department of Integrative Biology, University of California, Berkley, California

* Corresponding authors: guyteichman@gmail.com, odedrechavi@gmail.com.

[#] These authors contributed equally

Abstract

Can processes occurring in one individual's nervous system influence the physiology of the descendants? Here we explored the provocative hypothesis that parents' sensation or perception of environmental cues can influence their offspring, extending across many subsequent generations. We show that in *Caenorhabditis elegans*, temperature perception on its own can induce transgenerational changes in RNAi factors, small RNAs, and the genes that they regulate. Moreover, we identified secreted factors that enable a pair of thermosensory neurons (AFD) to communicate with the germline and trace the path of the epigenetic signal. We further modeled the process mathematically and validated the new predictions generated by the model experimentally. Hence, our results demonstrate that sensory perception is sufficient to trigger small RNA-mediated heritable gene expression memory.

Introduction

The nervous system is unrivaled in its ability to gather, process, and integrate information about the environment. Using data collected from sensory and internal organs, neurons orchestrate behavioral and physiological responses and prime future decisions, shaping the organism's response to environmental cues. In this study, we sought to test the provocative hypothesis that perception - the interpretation of sensory information - not only influences decision-making and physiology within the same generation but also generate long-term, heritable epigenetic memory transmitted across generations. Such a mechanism may be adaptive, although carry-over of aberrant epigenetic information may also be neutral or have negative consequences on health and survival of the animals [1–4].

C. elegans is a powerful model organism, offering unique advantages for investigating potential links between the nervous system, the germline, and inheritance. Thanks to the deterministic development of their nervous system, consisting of only 302 neurons, and their mapped neuronal connectome [5–8], these worms enable studying the nervous system at the circuit and single neuron levels. Moreover, *C. elegans* possess a vast array of small RNA-controlled processes [9,10] and, contrary to the longstanding dogma that DNA being the sole hereditary materials, have shown to be capable of inheriting small RNA responses and regulate germline gene expression transgenerationally [11,12].

Small RNA inheritance in *C. elegans* is achieved owing to the active amplification of small RNA responses by the RNA-dependent RNA polymerases (RdRPs) RRF-1 and EGO-1 [13–18].

Exogenous and endogenous siRNAs may trigger systemic gene silencing [11,19–23] and a suite of Argonaute proteins regulate the establishment and maintenance of this response [24,25,34,26–33].

Environmental stimuli play a role in regulating the synthesis and inheritance of small RNAs. For example, it has been shown that viral and bacterial infections [13,35,36], starvation [37–40], and changes in temperature [39,41,42] can modify the worms' small RNA pools transgenerationally. In particular, some germline-expressed transgenes undergo accumulative transgenerational epigenetic silencing when worms are grown at 20°C (a non-stressful temperature), but become re-expressed when worms are grown at 25°C (a mildly stressful temperature) [43–45]. Importantly, whether or not the different above-mentioned heritable effects of environmental challenges involve the action of the nervous system is unclear. More specifically, it is unknown whether the effects of temperature on transgene silencing is mediated by specific neuronal thermosensation pathways or by general physiological temperature responses.

Perception occurs following the activation of sensory neurons in response to specific stimuli. The received information is interpreted, inducing changes in behaviors, metabolism, or development that allow the animals to adapt to novel environments. In *C. elegans*, temperature sensation in the non-noxious range is mediated mainly by the AFD pair of sensory neurons [46–48], with additional contributions from the AWC, ASI and ASJ neurons [49–51]. Both the AFD and the AWC sensory neurons are postsynaptically connected to the AIY interneurons via chemical synapses [8], and the AIY, together with other downstream neurons, mediate thermotaxis behavior [48,52]. The AFD thermosensory circuit is capable of detecting both temperature changes [53,54] and long-term ambient temperature [55]. Multiple groundbreaking studies have shown that the AFD thermosensory neurons participate cell-nonautonomously in

long-term physiological responses to temperatures. AFD activation was shown to be sufficient to induce somatic expression of the transcription factor Heat Shock Factor-1 (HSF-1) [56], which partakes in the heat-shock response [57] and promote longevity at 25°C [58–60].

Previous studies suggest that certain neuronal processes that initiate in parents could continue to affect their F1 progeny [61]. For example, parental exposure to pheromones was shown to affect the children's reproduction and developmental rates [62]. However, these effects did not last beyond the F1 generation – an exemplar of *intergenerational* inheritance lasting a single generation, as opposed to perduring *transgenerational* inheritance that affects descendants not directly exposed to the original trigger (for example *in utero* exposure)[63]. In contrast, recent studies have demonstrated that endogenous small RNAs synthesized in neurons can affect gene expression and behavior transgenerationally (=> 3 generations) in *C. elegans* [21] and that neuronal hairpin-derived dsRNA can be transmitted to the germline and induce transgenerational gene silencing [19]. Still, a causal relationship between brain activity or sensory perception and transgenerational small RNA inheritance is yet to be established.

In this work, we used multiple independent experimental systems, coupled with computational modeling, to separate the direct biophysical effects of ambient temperature from its neuronal perception. Our findings reveal that the neuronal perception of temperature via AFD neurons, on its own, plays a pivotal role in governing transgenerational small RNA inheritance by controlling the expression of small RNA machinery in the germline. This neuronally mediated regulation of small RNA machinery depends on the secretion of the neuropeptide FLP-6, serotonergic signaling, and the transcription factor HSF-1. Our findings

imply that sensory perception regulates transgenerational inheritance of gene expression memory, which may influence the animal's survival fitness in changing environments.

Results

Disrupting AFD functions delays transgenerational gene silencing kinetics

To study whether temperature perception can affect inheritance, we first investigated the effect of AFD-mediated temperature perception on temperature-dependent transgene silencing. We used worms that carry a low-copy integrated *gfp* transgene expressed in the germline under the control of a germline promoter (*bnIs1*[*pie-1p::gfp::pgl-1*; *unc-119*(+)], which were previously described [64,65] (see **Figure 1A** and **Methods**). This transgene is constitutively silenced at 20°C. However, we observed that growing the worms at elevated temperature (25°C) for 1-2 generations rapidly and robustly triggered *gfp* expression from the transgene (**Figure 1B**). Shifting the worms back to low temperatures (20°C) resulted in a gradual, cumulative silencing response over 3-7 generations (**Figure 1C**). This heritable silencing response depends on small RNA inheritance as it was abolished in mutants lacking *hrde-1*, a gene encoding an Argonaute protein required for germline nuclear RNAi and many heritable small RNA-controlled processes [26], when raised at 20°C (**Supplementary Figure 1**).

We employed multiple complementary methods to disrupt AFD-mediated temperature sensation. These include ablating the AFD neurons, inducibly changing their membrane potential, or knocking out different AFD-specific genes required for temperature sensation, acclimation, or signal transduction to downstream neurons. In a typical experiment, we raised

both wild-type and different mutant worms at 25°C to achieve full transgene expression in the entire population. To track the dynamics of the temperature-dependent transgene silencing, we transferred wild-type and mutant worms to 20°C and monitored the expression of the germline transgene over at least three generations.

First, we noted that it took longer for the transgene to get transgenerationally silenced in worms that expressed a reconstituted caspase under the control of AFD-specific *gcy-8* promotor [48] (**Supplementary Figure 2**), providing a clue that AFD temperature sensation could affect germline small RNA-mediated silencing in a cell-nonautonomous manner. However, the transgenic worms expressing the caspase were sick and exhibited severe reduced brood size at both 20°C and 25°C. Hence, we deemed this AFD-disruption method suboptimal and proceeded to examine the AFD neurons' role in heritable gene silencing using alternative methods. To further examine the impact of AFD neuronal activity on temperature-dependent transgene silencing, we utilized the *Drosophila* histamine-gated chloride channel HisCl1 to reversibly hyperpolarize the AFD neurons [66,67]. We generated three independent lines expressing HisCl1 under the control of AFD-specific *gcy-8* promoter (see **Methods**). Worms carrying AFD:HisCl1 experience hyperpolarization of the AFD neurons when exposed to exogenous histamine (**Supplementary Figure 3A**). We then examined the impact of chronic HisCl1-driven AFD silencing, maintained through histamine supplementation, on temperature-dependent small RNA-mediated transgene silencing. We found that AFD:HisCl1 worms grown on histamine exhibited delayed silencing dynamics of the GFP reporter (**Figure 1D; Supplementary Figure 3B)**. While the wild-type control groups exhibited the expected progressive silencing of the GFP reporter over the course of 3-6 generations, the experimental group maintained stable GFP

expression in the population for at least 7 generations (**Figure 1D; Supplementary Figure 3B)**. It is noteworthy that AFD:HisCl1 worms not exposed to histamine exhibited an intermediate effect between the experimental group and the wild-type control groups. This may be a result of "leakiness" of the HisCl1 channels, even in the absence of histamine, which has been previously reported [68]. Taken together, these results suggest that disrupting AFD activity delays small RNA-mediated gene silencing.

Next, we examined whether the effect we observed is specific to the AFD neurons or caused by external factors such as the presence of an extrachromosomal array, stress response induced by the high-copy HisCl1 channels, or other non-specific effects on the nervous system. To that end, we generated a worm strain carrying a similar genetic construct expressing HisCl1 under the control of ASK-specific *sra-7* promoter, replacing the AFD-specific *gcy-8* promotor [69]. Like the AFD neurons, the ASK neurons are a symmetric pair of amphid head-sensory neurons. Unlike the AFD neurons, however, the ASK neurons are not known to respond to temperature stimuli or share direct synapses/gap junctions with other temperature-sensing neurons (ASK neurons are among the few known to not respond to temperature stimuli; see **Supplementary Table 1** summarizing current knowledge about the involvement of different sensory neurons in temperature sensation). We observed that ASK:HisCl1 had no effect on temperature-dependent gene silencing, regardless of the presence of exogenous histamine (**Supplementary Figure 3C**).

To further investigate our hypothesis regarding the "leakiness" of the HisCl1 channels, we attempted to engineer a worm strain expressing AFD:HisCl1 at a much lower level using a single-copy insertion (*SC-AFD:HisCl1*, see **Methods**). We reasoned that lowering the expression

level would mitigate the leakiness we observed in untreated worms, while still preserving some sensitivity to exogenous histamine treatment. However, we could not observe any transgene silencing effect in response to exogenous histamine treatment in SC-AFD:HisCl1 worms (**Supplementary Figure 4**), possibly because single copy of the channel is not potent enough to cause substantial hyperpolarization of the neurons. Indeed, it is important to note that in all previous published studies the channel was expressed in high-copy number [66–68,70].

To better assess the transgenerational effects of short-term vs. chronic AFD hyperpolarization, we investigated whether the effects of histamine treatment exhibit a dose-response relationship over generations. To that end, we used the experimental setup described above, however, in every generation of the experiment, we split some of the histamine-treated worms into a different experimental group, which we no longer treated with histamine. Those groups were termed "split" groups, and numbered according to the generation in which we split them from the histamine-treated parent group (see **Supplementary Figure 5A** for an illustration of the experimental design).

We found that histamine treatment of AFD:HisCl1 worms for one generation was sufficient to delay transgene silencing for the subsequent two generations, similar to worms that were grown on histamine for 2-4 generations and those that were exposed through the entire course of the experiment (**Supplementary Figure 5B**). This response was apparent even after two generations without histamine exposure and did not appear to increase in magnitude with longer exposure beyond two generations of histamine treatment.

Next, we examined whether the effect on small RNA-mediated gene silencing is transgenerationally inherited, persisting even when the AFD:HisCl1 construct is no longer present. To that end, we tested worms whose ancestors carried the AFD:HisCl1 construct for multiple generations (4 generations at 20°C, F1-F4) and then monitored them for multiple generations once they no longer carried the AFD:HisCl1 construct (the arrays are lost spontaneously in ~30% of the worms as confirmed by PCR, see **Methods**) (see **Supplementary Figure 6A** for an illustration of the experimental design). We found that AFD:HisCl1 induces changes in temperature-dependent small RNA-mediated transgene silencing that lasts for at least 3 generations after losing the construct, establishing that temperature sensation via AFD induces transgenerational changes in germline gene expression (see **Supplementary Figure 6B).** Taken together, these results imply that short term (1 generations) manipulation of activity in the AFD neurons can cause long-term (> 3 generations) transgenerational expression memory mediated by small RNAs in the germline.

AFD-controlled thermosensation regulates germline small RNA-mediated gene silencing

To further test our previous conclusions, we proceeded to investigate the impacts of temperature perception on small RNA-dependent gene silencing using a non-transgenic model, avoiding all possible unanticipated effects from introducing high-copy number of foreign DNA, which could potentially affect epigenetic processes. To that end, we examined many different genetic mutants with abolished temperature responses in the AFD neurons. We first examined triple mutants carrying null mutations in the three genes encoding AFD-specific guanylyl

cyclases *gcy-8*, *gcy-18*, and *gcy-23* (henceforth referred to as "AFD triple mutants" for brevity). These individual guanylyl cyclases are partially redundant but knocking out all three factors completely eliminates thermosensation in the AFD neurons [71–73]. When comparing the temperature-dependent silencing dynamics of AFD triple mutants and wild-type worms, we found that the AFD triple mutants showed a delayed temperature-dependent silencing response over multiple generations (**Figure 1E** and **Supplementary Figure 7A**), in agreement with the phenotypes of AFD ablated worms and animals carrying AFD:HisCl1. Notably, these three guanylyl cyclases are expressed *exclusively* in the AFD neurons [74–76], indicating that temperature sensation in the AFD neurons in particular affects heritable small RNA silencing, consistent with our previous findings. It is important to note that, while our results support the role of AFD activity in regulating epigenetic inheritance, we cannot rule out that other sensory neurons can also contribute to this process (see below).

Thermosensation controls germline small RNA-mediated gene silencing via neuropeptide signaling

To understand the mechanisms through which temperature perception affects heritable gene silencing responses in the germline, we examined additional mutants that lack components downstream to GCY-8/18/23 (**Figure 2A**). We started by inspecting mutants defective in the gene *cmk-1/CaMKI*. CMK-1 is a calcium/calmodulin-dependent kinase expressed primarily in sensory neurons, and most prominently in the AFD neurons. In fact, compared to other neuronal classes, AFD exhibits both the highest *cmk-1* level and constitutes

the largest fraction of isolated cells that express *cmk-1* based on the CeNGEN single cell sequencing dataset (see **Supplementary Figure 8A**) [76]. CMK-1 is required for long-term temperature adaptation in the AFD neurons [55,77,78]. We found that mutants of *cmk-1* exhibited a defective transgenerational silencing response, similar to AFD triple mutants (**Figure 2B** and **Supplementary Figure 7B**).

Previous studies have shown that CMK-1 can phosphorylate the CREB homolog CRH-1 at the serine 48 residue [58,79]. Moreover, it was demonstrated that CMK-1 phosphorylates CRH-1 in the AFD neurons in a temperature-dependent manner, promoting the expression of the neuropeptide-encoding gene *flp-6* [58,80]. FLP-6 subsequently mediates communication between the AFD thermosensory neurons and the AIY interneurons [58]. We therefore hypothesized that the AFD-AIY thermosensory circuit could regulate temperature-mediated gene silencing in the germline. When examining mutants of *flp-6*, we found that they exhibited a defective transgenerational transgene silencing response to low ambient temperatures, similar to that of AFD triple mutants (**Figure 2C** and **Supplementary Figure 7C**). This phenotype persisted for at least 10 generations following the transition to 20°C (see **Supplementary Figure 8B**). The prolonged de-silencing of transgenes in *flp-6* mutants, which was longer-lasting than that observed in AFD triple mutants, suggests the potential involvement of other neurons in this process (see **Discussion**).

Taken together, our results suggest a model whereby CMK-1, functioning downstream of GCY-8/18/23 in AFD, activates neuropeptide FLP-6, which leads to transgenerational silencing of germline transgene.

Change in ambient temperatures and HSF-1 activity affect small RNA inheritance in both sensation-dependent and -independent manners

HSF-1, a conserved transcription factor involved in development and stress response, has previously been shown to determine the epigenetic "inheritance state" of worms by regulating small RNA factors in the germline [25]. In particular, low activity of HSF-1 reduces small RNA-dependent silencing of transgenes and RNAi inheritance, while HSF-1 over-expression supports small RNA-mediated gene silencing. Moreover, the AFD neurons have been shown to regulate germline activation of HSF-1 cell-nonautonomously through serotonergic signaling mediated by serotonin receptor SER-1 [57,59]. We therefore hypothesized that HSF-1 may similarly regulate the effects of neuronal sensation on small RNA inheritance.

To investigate the involvement of serotonin release in small RNA-mediated gene silencing, we examined whether mutants of the tryptophan hydroxylase *tph-1* or the serotonin receptor *ser-1* show modified temperature-dependent transgene silencing. We found that *tph-1* mutants exhibited a strong delayed heritable transgene silencing (**Figure 2D** and **Supplementary Figure 7D**), persisting for at least 10 generations following the transition to 20°C (see **Supplementary Figure 8C**). However, we could not detect any difference in heritable transgene silencing in *ser-1* mutants (**Supplementary Figure 9**). These results suggest that, while serotonin mediates the effects of AFD thermosensation on germline small RNA-mediated gene silencing, other serotonin receptors, either instead of or in addition to SER-1, are involved.

Next, to investigate the involvement of HSF-1, we examined the temperature-dependent silencing dynamics of *hsf-1* partial loss-of-function mutants (*hsf-1* null mutants are lethal [81–83]). Since *hsf-1* mutants are hypersensitive to heat stress (they die at 25°C), we conducted these experiments within a narrower temperature range (20-22°C). We found that -*hsf-1* mutants display a delayed silencing phenotype reminiscent of *flp-6* and *tph-1* mutants (**Figure 2E** and **Supplementary Figure 7E**). These results indicate that heritable transgene silencing in the germline depends on serotonin release, likely from ADF and NSM downstream of AFD in the thermosensory circuit, as well as HSF-1 activity in the germline (more below).

Mutants of *cmk-1*, unlike other sensory mutants, exhibit a high-variance gene silencing response at high ambient temperature

Intriguingly, in all mutants that we examine, other than *cmk-1*, we observed defective transgenerational silencing only when the worms were transitioned in one direction - from high (25°C) to low temperatures (20°C) (**Figure 2** and **Supplementary Figure 7**). When we transitioned the worms from low temperature (20°C) to high temperature (25°C), we did not detect any difference between wild-type worms and *tph-1*, *flp-6*, and *gcy-8/18/23* mutants (**Figure 2F-I** and **Supplementary Figure 7F-I**), with all strains achieving near-complete de-silencing of the GFP reporter within 2-3 generations.

In *cmk-1* mutants, on the other hand, we observed a very interesting and unusual high-variance response when transitioning from low to high temperature: some worm lineages exhibited rapid de-silencing of the GFP reporter, others maintained complete silencing for at

least 7 generations, and still others repeatedly fluctuated between the two extremes (**Figure 2G, Supplementary Figure 7G,** and **Supplementary Figure 10**). This suggests that different factors, perhaps in neurons outside of AFD, coordinate the responses to changes in temperature, depending on whether the worms transition up or down the temperature gradient (see **Discussion**).

Characterizing the effects of neuronal temperature sensation on the composition of the endogenous heritable small RNA pool

Our foregoing results demonstrate that AFD thermosensory circuit has a major impact on transgenerational transgene silencing at different temperatures; we then sought to further explore the small RNA responses to changes in ambient temperature. Thus, we used RNA sequencing to characterize the differences in gene expression and heritable small RNAs in worms with defective temperature sensation at multiple stages of the sensory pathway.

First, we characterized the changes in small RNA pools cloned from wild-type and AFD triple mutant (*gcy-8/18/23*) day 1 adult worms across multiple generations during the transition from a high temperature (25°C) to a low temperature (20°C) (see experiment summary in **Figure 3A** and detailed experimental plan in **Methods**). We found that, in accordance with the cumulative silencing phenotype we observed upon temperature transition, anti-*gfp* siRNAs appear to accumulate over generations (**q = 0.058981**), with overall higher levels in wild-type worms compared to AFD triple mutants (**Figure 3B**, **q = 0.08163**). Interestingly, this accumulation does not appear to be linear, as the level of anti-*gfp* small RNAs modestly

decreases in the first generation at 20°C before significantly increasing in the subsequent generations.

We identified two groups of siRNAs targeting protein-coding genes that significantly accumulate over generations at 20°C based on their transgenerational accumulation dynamics (see **Figure 3C** and **Methods**). Interestingly, both groups showed significantly slower transgenerational accumulation in AFD triple mutants compared to wild-type worms (**Figure 3D**). We found that the first group is enriched for small RNAs associated with the germline Argonautes HRDE-1, PPW-1, PPW-2, and WAGO-1, as well as the ubiquitous Argonaute NRDE-3 (**Figure 3E – left panel**). The second group, whose accumulation pattern resembled that of anti-GFP siRNAs, is similarly enriched for small RNAs bound to the germline-specific Argonautes HRDE-1, PPW-1, PPW-2, and WAGO-1 (**Figure 3E – right panel**).

In summary, our findings reveal a transgenerational accumulation of siRNAs targeting specific genes, including the *gfp* transgene, following the transition from high to low temperatures. This accumulation appears more pronounced in wild-type worms compared to AFD triple mutants and the small RNAs tend to associate with specific germline Argonautes, suggesting that the perception of temperature can transgenerationally modulate the composition of heritable small RNA pools in the germline.

Next, given the unusual gene silencing behaviors of *cmk-1* mutants compared to other sensory mutants we analyzed, we sought to characterize the high-variance response that we observed in *cmk-1* mutants upon transition from low to high temperatures (**Figure 2G** and **Supplementary Figure 10**). To that end, we sequenced small RNAs and mRNAs from wild-type

and *cmk-1* worms before and after transitioning from a low temperature (20°C) to a high temperature (25°C). For the mutant worms, we isolated both "expressing" lineages (i.e., lineages in which GFP silencing was abolished at high temperature) and "silencing" lineages (i.e., lineages in which GFP silencing was maintained at high temperature) (see **Figure 4A** and **Methods**).

Interestingly, in the small RNA data sequenced from the P0 generation (20°C), we did not detected changes in anti-*gfp* siRNA levels between "expressing" and "silencing" lineages (**Supplementary Tables 2)**. In F3 (25°C), however, we detected differences in anti-*gfp* siRNAs (**Figure 4B-C, q < 0.006**), as well as changes in small RNAs known to be associated with specific Argonautes (**Supplementary Tables 4 and 5**). These results indicate that the bimodal silencing phenotypes we observed in *cmk-1* mutants emerges only after the transition to a high temperature and cannot be directly predicted from the small RNA pools of the P0 ancestors.

In agreement with the reduction in the gene silencing capacity we observed in *cmk-1* mutants, we detected a significant reduction in the fraction of siRNAs targeting protein-coding genes in *cmk-1* mutants grown in both 20°C and 25°C (**Figure 4D**)**.** Interestingly, while piRNAs were downregulated in wild-type worms upon transition to high temperatures, as previously shown [44], *cmk-1* showed an upregulation of piRNAs (**Figure 4E**), which may explain the high-variance stochastic silencing response in the mutants at 25°C (see below).

We next proceeded to analyze the changes in the pools of endogenous siRNAs following changes in ambient temperature. We found siRNA changes that are both sensation-dependent (i.e., occur in wild-type worms but not in *cmk-1*) and -independent (i.e., common to both wild-

type worms and *cmk-1*) (**Figure 4F**). While the siRNAs changing in a sensation-independent manner were not enriched for targets of particular Argonaute proteins, we found that siRNAs downregulated in a sensation-dependent manner were enriched for small RNAs bound to the ubiquitous Argonautes SAGO-1, SAGO-2, and NRDE-3, as well as the germline-specific Argonautes PPW-2 and WAGO-1 (**Figure 4G**) [30]. Moreover, we found that siRNAs upregulated in a sensation-dependent manner were enriched for CSR-1- and WAGO-4-bound small RNAs, which were previously shown to target a similar cohort of constitutively-expressed germline genes [30,84,85]. Of particular interest, WAGO-4 has previously been found to mediate transgenerational epigenetic inheritance [84,86]. Additionally, CSR-1 is thought to protect germline mRNAs from piRNA silencing, which may be enhanced in *cmk-1* (**Figure 4E**) [85,87–89].

All together, these results indicate that, while high temperatures can non-specifically disrupt small RNA-mediated gene silencing, the neuronal perception of ambient temperature may regulate specific small RNA pathways in the germline.

We then proceeded to examine changes in gene expression in response to changes in ambient temperature and its perception. When examining the mRNA sequencing data, we found that a large group of epigenetic factors, comprising multiple Argonaute genes (including the germline-specific Argonaute genes *hrde-1*, *wago-1*, *wago-4*, and *ppw-1*), as well as multiple RNA-dependent RNA polymerase genes (*rrf-1, rrf-3,* and *ego-1*), are significantly downregulated at high temperatures in wild-type animals. All of these genes are chronically downregulated in *cmk-1* mutants (**Figure 5A-B** and **Supplementary Table 3**); however, we did not detect any significant differences in gene expression between the GFP-silencing and GFP-expressing lineages *of cmk-1* at the mRNA levels, despite changes in the siRNA pools (see **Supplementary**

File 2). Importantly, we observed a similar trend of downregulation in epigenetic genes when examining the mRNA sequencing data of AFD-ablated worms (**Figure 5C** and **Supplementary Table 3**) [60], suggesting that the sensation of high temperature, particularly in AFD, reduces the capacity of the small RNA machinery.

Remarkably, we found that many of these small RNA factors (75 out of 312 epigenetic genes) are similarly downregulated following germline-depletion of HSF-1 (**Figure 5D** and **Supplementary Table 3**) [90], further supporting the involvement of germline HSF-1 in the small RNA response to temperature sensation.

In summary, while exposure to high temperature appears to disrupt worms' small RNA pools in a non-specific manner, the perception of temperature alone leads to targeted changes in the composition of small RNAs. Of note, AFD disruption leads to downregulation of epigenetic factors, which may subsequently impair germline siRNA-mediated gene silencing. The overlapping transcriptional signatures observed in *cmk-1* and AFD-ablated worms suggest that AFD-mediated temperature sensation elicits specific epigenetic responses in the germline, although other neurons may also play a role.

Predicting the impact of changes in ambient temperatures and sensory input on small RNA-mediated gene silencing

Multiple theoretical models have been proposed to explain the dynamics of transgenerational inheritance of epigenetic information [24,25,91,92]. To further explore the impact of temperature and temperature perception on transgenerational inheritance, we expand upon

the recently published mathematical model developed by Karin et al. [92] (see **Figure 6**, **Supplementary file 1** and **Methods** for the detailed assumptions and parameters of the model).

Our revised model makes three additional assumptions based on our RNA sequencing data: (1) high temperatures (or defective temperature perception) reduce the silencing capacity of the worms; (2) the *gfp* reporter gene is targeted by stochastic silencing events at a high frequency; and (3) the frequency of stochastic silencing events against *gfp* is reduced by high temperatures (or *cmk-1* loss-of-function).

Our simulations show that the model predicts the empirically observed kinetics of *gfp* silencing following temperature transitions: a rapid, uniform de-silencing response upon transition from low to high temperature (**Figure 6C**), and a stochastic and cumulative silencing response upon transition from high to low temperature (**Figure 6B**). Moreover, in agreement with our RNA sequencing results, our simulations suggest that a perception-dependent reduction in silencing capacity is sufficient to explain the reduced transgene silencing phenotype we observed in multiple temperature sensory mutants (see **Figure 6B-D** for simulated results; see also **Figure 2** for experimental results).

More importantly, a new prediction was raised by our theoretical model: worms defective in temperature sensation should be deficient in the inheritance of all RNAi responses, including exogenous, target-specific, dsRNA-induced RNAi, even in the absence of temperature changes and regardless of stochastic silencing responses (**Figure 7A**). We proceeded to test this prediction and examine the potency of RNAi inheritance in worms defective in temperature sensation. We exposed wild type and *cmk-1* mutants carrying germline GFP (*mjIs134[mex-*

5::GFP]) to anti-*gfp* dsRNA and monitored the inheritance of GFP silencing. We found that, while the basal expression *mex-5::GFP* remains unchanged in *cmk-1* mutants (**Supplementary Figure 11A)**, these mutants are heritable RNAi deficient ("*Hrde*"), even at normal temperature (20°C) (**Figure 7B** and **Supplementary Figure 11B**). This, and our previous results, strongly demonstrate that neuronal temperature perception alone, independent of the actual temperature or the biophysical effects of heat, could modify transgenerational inheritance of epigenetic information.

Discussion

In this study, we found that perception of temperature via the AFD neurons affects germline small RNAs cell-nonautonomously, influencing the dynamics of transgenerational epigenetic inheritance. AFD controls the expression of small RNA factors, including Argonaute proteins and RdRPs, as well as heritable RNAi through FLP-6 neuropeptide and serotoninergic signaling, which directly or indirectly affects the activity of transcription factor HSF-1 in the germline (**Figure 7C**).

In this manuscript, we used three different model systems to interfere with neuronal perception of temperature: an ablation model, a chemogenetic model, and genetic knockout models. Each of these models has inherent weaknesses. Neuron ablation is an aggressive procedure that may induce additional stress responses in the worms. Indeed, these worms are sick and infertile. The chemogenetic model suffers from "leakiness", complicating its study. The knockout models, and in particular the triple mutants lacking three AFD-specific guanylyl

cyclases that we used in many assays, are not inducible. Despite these individual weaknesses, however, the complementary nature of these diverse approaches provides a robust framework for investigation. The similarity of outcomes across different model systems, as well as between the many additional mutant strains that we used to examine different stages of the thermosensory circuit, strengthen our conclusion that thermosensation non-cell autonomously affects germline Argonaute activities, leading to heritable gene expression memory. In addition to AFD, it is likely that other sensory neurons are involved in promoting germline gene silencing. Supporting this notion, animals lacking *flp-6*, which is expressed in other amphid neurons outside of AFD, including ASE and ASG neurons [93], showed a stronger a phenotype than AFD triple mutants. Similarly, knocking out *cmk-1*, which is expressed in multiple neuronal types [77], causes a bistable expression pattern when the mutants were transferred from low to high temperature – a phenotype absent in other thermosensory mutants we analyzed in this work.

This work supports our previous finding on the roles of HSF-1 in regulating heritable small RNA responses [25] . We showed that disrupting AFD thermosensation and eliminating HSF-1 relief epigenetic silencing in the germline. Previous studies have demonstrated that HSF-1 has at least two roles – a developmental program and a stress-response program - both of which compete for HSF-1 binding [90,94,95]. While we did not focus on the molecular details of HSF-1 regulation in this manuscript, other works have indicated that HSF-1 binds the promoters of some epigenetic genes under non-heat shock conditions [90]. Consistently, we found that germline-specific depletion of HSF-1 causes downregulation of genes encoding Argonautes and other epigenetic regulators. Future studies are required to understand how HSF-1 and the small RNA machinery co-regulate development and stress responses.

In this work, we zeroed in on the perception of temperature due to the profound roles temperature play in development, reproduction, and aging [58,96–98]. However, other neuronally perceived stimuli - such as other types of stress, positive cues, or even neuronally-controlled learned behaviors - may be able to affect small RNA silencing, similar to the effects of temperature we reported here. Our approach - disrupting the function of specific neurons using complementary strategies and characterizing environment-sensitive transgenerational silencing of specific genes - offers a straightforward paradigm for studying neuron-to-germline communication in regulating inheritance. Future research could aim to decipher the neuronal 'code' that modulates epigenetic inheritance and characterize its physiological relevance.

It is likewise possible that different regimes of temperature stimuli, such as low temperature exposure (12-19°C), a transient heat shock, or recurring temperature fluctuations, may have different repercussions on small RNA inheritance. For example, our previous work has shown that a 2-hour heat shock is sufficient for “resetting” of ancestral small RNA responses [99]. In this work, we focus on the effects of prolonged (> 5 generations) exposure to elevated temperature; future research could explore the consequences of fluctuating environments on the worms’ small RNA pool and transgenerational epigenetic inheritance.

Why would worms actively repress small RNA pathways when exposed to high temperatures? Reducing epigenetic regulation could constitute a mechanism for increasing genetic and phenotypic variability in largely isogenic population. *C. elegans* can distinguish between self and non-self genes, actively repressing foreign elements using heritable small RNAs [33]. In normal conditions, the activity of small RNA machinery is required for maintaining genome stability and preventing the harmful effects of transposition. When faced with stress,

on the other hand, inhibition of the small RNA machinery may induce phenotypic plasticity and/or novel genetic variants, potentially allowing the animals to adapt to the environments [100]. Indeed, while in this study we focused on how temperature perception controls transgenerational epigenetic regulation, an accompanying paper reports that AFD dysfunctions leads to mobilization of transposable elements in the germline, which may serve as building blocks for genetic novelty [84,86].

The nervous system of *C. elegans* in general, and the AFD neurons in particular, were shown to mediate a variety of cell-nonautonomous processes [56–58,101–105]. Persistent epigenetic memory of temperature stress in the absent of the initial trigger has been shown to have a negative fitness cost, at least under laboratory conditions [44]. It is tempting to speculate that intact thermosensation is required for re-calibration of the epigenetic states, allowing animals to readily adapt to new environments and promote the survival fitness of future generations – an intriguing model that warrants future investigation. In summary, the findings of this study illuminate a novel mechanism by which neuronal activity could control gene expression non-cell autonomously and direct non-Mendelian inheritance.

Materials and Methods

Worm cultivation

We used standard culture techniques to maintain the nematodes. We grew the worms on Nematode Growth Medium (NGM) plates and fed with OP50 bacteria. We took extreme care to avoid contamination or starvation for at least five generations prior to each experiment. We discarded contaminated or starved plates from the experiments. We performed all experiments with at least three biological replicates. We indicated all of the nematode strains we used in this study in the Key Resources Table.

Histamine treatment

In experiments where worms were treated with histamine, we added a sterile-filtered 1M solution of histamine dihydrochloride to NGM agar at 50°C immediately before pouring the plates, to a final concentration of 10mM [66]. We stored histamine plates in 4°C for up to a month before usage.

In experiments where worms lost the HisCl1 extrachromosomal construct, we validated that all P-1 parents of worms lost the construct via PCR amplification of the HisCl1 construct, discarding any plate that showed residual presence of HisCl1.

Fluorescence microscopy

For fluorescent microscopy assays, we used either an *Olympus IX83* motorized inverted wide-field microscope, or an *Olympus BX63* motorized upright wide-field microscope. We imaged experiments with a 10X objective lens, with an exposure time of 1000ms for GFP and 1500ms for mCherry.

Generally, we picked worms onto a microscope slide with 2% agarose pad containing drops of levamisole to induce paralysis, covered them with a glass coverslip, and imaged them after 2-5 minutes.

Scoring of germline GFP reporter silencing

We scored GFP silencing and inheritance using a binary system: no visible expression (OFF), or any level of expression (ON). The results of each experimental group within each biological replicate were summarized as the percentage of worms showing any GFP expression, out of the entire worm population ($\frac{ON}{ON+OFF} * 100$). The experimenters were blinded to the experimental conditions while scoring the experiments using *DoubleBlind* [106].

In experiments and experimental conditions expressing HisCl1 constructs, we discarded worms that exhibited a non-specific expression pattern or no visible expression in the appropriate neuron pairs from the analysis.

In experiments where we quantified the basal expression level of GFP (**Supplementary Figure 11A**), we used the ImageJ Fiji 'measure' function [107] to measure the integrated density of the three germline nuclei closest to spermatheca in each worm, as well as a mean

background measurement of the worm in the germline's vicinity. If less than three germline nuclei were visible, we took the remaining measurements in the estimated location and size of the germline nuclei instead. We calculated the corrected total cell fluorescence (CTCF) of each germline nucleus as previously described [108]. We used the mean of all three CTCF scores as the worm's fluorescence score, and normalized the scores of each biological replicate to the mean of the control condition in that biological replicate.

Since some genetic background/experimental conditions can lead to developmental delays, worms in different conditions sometimes reached adulthood in different days. To avoid age bias between the different conditions, we tracked the developmental stages of all worms, and imaged them when they reached the 'day-one adulthood' stage.

Statistical analysis

For transgenerational silencing experiments, we analyzed the data using a mixed effect model, with the genotype/treatment considered as a categorical factor, and the generation considered as repeated-measures data. We then followed up with multiple comparisons, comparing the means of the experimental conditions to the mean of the control condition within each generation.

In experiments with exactly two conditions (experimental vs control), we used the Unpaired Student's t-test with Welch's correction for unequal variances. For experiments with multiple conditions and/or generations, we corrected for multiple comparisons using the Two-stage step-up method of Benjamini, Krieger and Yekutieli [109].

mRNA and small RNA sequencing experiments

Collecting worms for sequencing

For the *gcy-8/18/23* mutant experiment, we raised wild-type and mutant animals in 25°C for at least 5 generations. We ran the experiment in three biological replicates, each containing 3-5 technical replicates. We initiated each technical replicate with 25 parent worms in the P-1 generations. After 2-3 hours of synchronized egg laying, we imaged the parent worms to ensure a uniform starting point of GFP reporter expression. We additionally imaged the worms in every generation, to keep track of the GFP expression phenotype of each technical replicate. We synchronized each new generations from 25 randomly selected parent worms. We isolated adult worms in the P0, F1, F2, and F3 generations.

From each biological replicate, we selected one wild-type and one mutant replicate, based on their GFP reporter expression in the F3 generation: we selected the replicate whose GFP expression was closest to its genotype's median GFP expression. We did this to ensure that the samples we chose were representative of the phenotype we observed in previous experiment, while avoiding selection bias.

For the *cmk-1* mutant experiment, we raised wild-type and mutant animals in 20°C for at least 5 generations. We ran the experiment in three biological replicates, each containing 8-10 technical replicates. We initiated each technical replicate with 25 parent worms in the P-1 generations. After 2-3 hours of synchronized egg laying, we imaged the parent worms to ensure a uniform starting point of GFP reporter expression. We additionally imaged the worms in the F2 generation, to keep track of the GFP expression phenotype of each technical replicate. We

synchronized each new generations from 25 randomly selected parent worms. We isolated adult worms in the P0 and F3 generations.

From each biological replicate, we selected two technical replicates to be sequenced based on their GFP expression in the F2 generations: we selected the worms with highest GFP expression ("expressing" samples), and the worms with the lowest GFP expression ("silencing" samples). We did this to ensure that we picked worms representing both extremes of the silencing phenotypes we observed in previous experiments and facilitate comparisons between worms that responded differently to changes in temperature.

RNA extraction

We performed RNA extraction as previously described [21]. We lysed worms using the TRIzol reagent. We added 400 ul of TRIzol to 100 ul of adult worms and performed three cycles of freezing in -80°C and vortexing at RT for 15 minutes. We added 100 ul of chloroform to the samples, transferred them to pre-spun Heavy Phase-Lock tubes, and rested them on ice for 10 minutes. Next, we centrifuged the tubes at 16,000 g for 15 minutes at 4°C. We transferred the aqueous phase to a second pre-spun Heavy Phase Lock tube, added 1:1 of a Phenol:Chloroform:Isoamyl Alcohol (25:24:1) mixture, and centrifuged the samples at 16,000 g for 5 minutes at RT. We transferred the aqueous phase to a 1.5 ml Eppendorf tube and added 20 ug of Glycogen and 1:1 Isopropanol. We incubated the samples at -20°C overnight, and then spun them for 30 minutes at 16,000 g at 4°C. We washed the resulting pellet twice with ice-cold 70 % ethanol and then air-dried for 10 minutes. We then re-suspended the pellet in 20 ul of

RNase-free water. We validated the concentration of the total RNA using Qubit RNA high-sensitivity kit, and ensured that the RNA integrity was sufficiently high (RIN >= 7) using an Agilent 4150 BioAnalyzer instrument and High Sensitivity RNA ScreenTapes.

mRNA libraries

We enriched the samples for poly-A-tailed mRNA molecules using the NEBNext Poly(A) mRNA Magnetic Isolation Module, using a starting quantity of 100-1000 ng Total RNA.

For the *cmk-1* mRNA samples, we generated cDNA libraries using the NEBNext Ultra II Directional RNA Library Prep Kit and the NEBNext Dual Index Primers multiplex oligos. We sequenced the libraries using an Illumina NextSeq 500 instrument.

Small RNA libraries

We treated total RNA samples with RNA 5' Polyphosphatase (LGC, Biosearch Technologies) to ensure 5' monophosphate-independent capture of small RNAs. We prepared small RNA libraries using the NEBNext® Small RNA Library Prep Set for Illumina® according to the manufacturer's protocol. We separated the cDNA libraries on a 4 % agarose E-Gel (Invitrogen, Life Technologies), and selected the 140-160 nt length bands. We pooled and purified the size-selected cDNA using the MinElute Gel Extraction kit (QIAGEN). We sequenced the libraries using an Illumina NextSeq 500 instrument.

RNA sequencing analyses

Sequencing analyses were done using *RNAlysis* [110], and all of the details of the analyses, including workflow, function parameters, graphs, and intermediate data, are available in **Supplementary Files 2-4 – RNA Sequencing Interactive HTML Report**.

For small RNA sequencing datasets, we used FastQC to assess sample quality [111], filtered out reads shorter than 15 nucleotides after adapter trimming using CutAdapt [112], aligned small RNA reads using ShortStack [113], and counted aligned small RNA reads using FeatureCounts [114].

For mRNA sequencing datasets, we used FastQC to assess sample quality, aligned reads using HISAT2 [115], and counted aligned reads using FeatureCounts.

Classification of groups of siRNAs that accumulate transgenerationally in 20°C

First, to identify groups of siRNAs whose expression changes significantly over generations in 20°C, we ran differential expression analysis using *Limma-Voom*, with the design formula "~ Genotype + poly(Generation, degree = 2)". We kept only siRNAs whose polynomial coefficients of the *Generation* parameter were significantly different from 0 ($q<0.1$).

Next, to group these siRNAs based on their change pattern, we filtered genes based on the values of their 1st and 2nd polynomial coefficients, keeping only those whose 1st and 2nd coefficients were larger than 0.5 or smaller than -0.5. We then examined the four possible combinations of coefficient ranges (1st/2nd, greater than 0.5/lesser than -0.5), and picked the two groups of siRNAs that exhibited transgenerational accumulation dynamics.

Mathematical model

We based our mathematical model on the Toggle-Inhibitor-Competition (TIC) model developed in Karin et al., 2023, which aimed to explain transgenerational inheritance of small RNA responses, as well as the similarities and differences in small RNA inheritance between isogenic worms. We expanded this model to apply to temperature-dependent small RNA-mediated gene silencing and simulated the effects of the changes in the model's parameters and components affecting this process.

Based on our experimental results, we aimed to fulfill the following requirements:

1. Change of growth temperatures modifies the small RNA responses of worms in both sensation-dependent and -independent manners.
2. The *gfp* reporter should acquire silencing gradually and stochastically when transitioned from high to low temperatures, but de-silence rapidly and uniformly when transitioned from low to high temperatures.
3. Worms defective in AFD temperature sensation show delayed accumulation of silencing in low temperatures, but de-silence normally in high temperatures.

Based on our mRNA and small RNA sequencing results, we made the following assumptions:

1. High temperatures, or defective temperature sensation, reduce the silencing capacity of worms ($\mathbf{V_{tot}}$) by ~two-fold. We base this on the observed downregulation of small RNA machinery genes in 25°C, and in worms defective in AFD temperature sensation (**Figure**

3). This is also supported by **Figure 3A** of **Houri-Zeevi et al., 2021**, which demonstrates that RNAi inheritance is reduced when worms are raised in high temperatures in the generation following RNAi.

2. To explain the RNAi-free accumulation of silencing in low temperatures, the *gfp* reporter gene must be targeted by stochastic silencing events at a higher frequency than other genes. According to our small RNA sequencing data, it is in the top 1% of small RNA-targeted genes – normalized siRNA levels are ~20-25 fold larger than that of the average protein-coding gene (**Supplementary Table 6**).
3. To explain the maintenance of near-100 % expression of the *gfp* reporter at high temperatures, the frequency of *gfp* silencing events must be reduced by high temperatures. This is possibly due to reduction in piRNA levels (and probably other factors), which we observed in our small RNA sequencing data (**Figure 4C**).

We then proceeded to simulate transgenerational-silencing experiments, where worms are transitioned from a higher temperature to a lower temperature, or vice versa. As in the "real" experiments, we started each simulated experiment with 25 random worm lineages, and randomly picked 25 worms at each generation (84 hours) to spawn the next generation of worms.

For the simulated RNAi experiment, we initiated an RNAi trigger as in Karin et al. 2023, with the entire simulation being conducted in a lower temperature, such that the silencing capacity (V_{tot}) of wild-type worms is ~2 times higher than in the mutants.

The simulation code is available online at github.com/GuyTeichman/Teichman_2024, as well as **Supplementary File 1 – simulation code**.

DNA constructs and transgenic animals

To express HisCl1 and GCaMP6 in the AFD neurons we used the AFD-specific promoter *gcy-8* [71]. An expression vector containing *gcy-8p::HisCl1::SL2:mCherry:unc-54 3'UTR* was generously gifted by the lab of Dr. Piali Sengupta. An expression vector containing *gcy-8p::GCaMP6:unc-54 3'UTR* was generously gifted by the lab of Dr. Daniel Colón-Ramos.

To improve the expression specificity of the construct, we replaced the *unc-54* 3'UTR sequence in both vectors was replaced with the *rab-3* 3'UTR sequence (656bp amplified from genomic DNA) via Gibson Assembly.

To express HisCl1 and GCaMP6 in the ASK neurons we used the ASK-specific promoter *sra-7* [69,76]. We amplified 4kbp upstream of the *sra-7* ORF from *C. elegans* genomic DNA following [69] using the primers ATAGCGGCCGCGAGAAATATTTGATGGATGTTTG (forward) and ATTGGGATCCCAAAAGTCAACGGACTGTGA (reverse), which also inserted the restriction sites for NotI and BamHI respectively. We used Phusion® High-Fidelity DNA Polymerase (NEB) to amplify the *sra-7* promoter using the company's protocol. We purified the resulting PCR product (QiaQuick PCR Purification Kit, Qiagen) and double-digested it using NotI-HF and BamHI-HF (rCutSmart buffer, NEB) following the manufacturer's standard procedure. We then purified the inserts (Qiaquick PCR Purification Kit, Qiagen).

We cut each of the vectors in a similar manner using the same restriction enzymes. We separated the resulting products in agarose gel (1 %) and purified them (Wizard SV Gel and PCR

Clean-Up System, Progema). We then ligated the inserts and vectors with Quick Ligase (NEB) following the company's standard procedure. We transformed the ligated constructs to TOP10 competent cells under selection using carbenicillin at 100 ug/ml (Sigma). After transformation, we extracted the plasmids (QIAprep Spin Miniprep Kit, Qiagen). We verified the plasmid sequences using Sanger sequencing with an M13 primer (AGCGGATAACAATTTCACACAGGA).

We injected the HisCl1 and GCaMP6 constructs into N2 worms, along with the co-injection marker *rol-6(su1006)* (pRF4) and DNA ladder (1kb DNA Ladder N3232, NEB), generating the three AFD-specific independent lines BFF95, BFF96, BFF97: *pigEx17/18/19*[*gcy-8p::HisCl1::SL2::mCherry::rab-3* 3'UTR + *rol-6p::rol-6(su1006)::rol-6* 3'UTR + *gcy-8p::GCaMP6::rab-3* 3'UTR], as well as ASK-specific line BFF126: *pigEx21*[*sra-7p::HisCl1::SL2::mCherry::rab-3* 3'UTR + *rol-6p::rol-6(su1006)::rol-6* 3'UTR + *sra-7p::GCaMP6::rab-3* 3'UTR].

We injected the constructs in the following concentrations: HisCl1 (25 ng/µl), GCaMP6 (25 ng/µl), pRF4 (25 ng/µl) and DNA ladder (25 ng/µl). We then crossed the various HisCl1 lines into worm strain SS747, which contains a GFP temperature-dependent silencing reporter.

Acknowledgements

We thank all members of the Rechavi lab and co-authors for fruitful discussions, feedback, and support. O.R. is grateful to funding from the Eric and Wendy Schmidt Fund for Strategic Innovation (Polymath Award #0140001000) and the generous support from the

Morris Kahn foundation. GT is grateful to the Milner Foundation. C.K.E is supported by EMBO Post-doctoral Fellowship (ATLF 6-2022). The Rechavi lab is funded by ERC grant #335624 and the Israel Science Foundation (grant#1339/17). O.R. and B.S. acknowledge funding from the John Templeton Foundation Grant (61734) and the Deutsche Forschungsgemeinschaft (project 437407415, SCHU 2494/10-1).

Author contributions

O.R conceptualized the idea for the project. G.T., M.S., and O.R. conceptualized and designed the experiments. G.T., C.K.E., M.S., H.D., and V.P., M.M and M.Sh conducted the experiments. I.R. and O.S. generated the DNA constructs. V.P. and M.O.S. conducted calcium imaging experiments. G.T. and C.K.E worked on Statistical Analysis, Data Curation, and Visualization. G.T. and H.G. ran bioinformatic analyses. G.T. modified the mathematical model and wrote the simulations. G.T., C.K.E., and O.R. wrote the manuscript with input from the other authors.

Declaration of interests

The authors declare no competing interests.

Data and Code Availability

The simulation code is available online at github.com/GuyTeichman/Teichman_2024 , as well as **Supplementary File 1 – simulation code**.

A complete report of RNA sequencing data analysis, including intermediate files and function parameters, is available as **Supplementary Files 2-4 – interactive analysis reports**.

Small RNA and mRNA sequencing libraries generated during this study are available at the GEO repository accession number GEO: [TBA]

We used the following previously published datasets:

Apfeld J (2022) NCBI BioProject ID PRJNA822361. Neuronal temperature perception induces specific defenses that enable *C. elegans* to cope with the enhanced reactivity of hydrogen peroxide at high temperature.

Li J (2021) NCBI BioProject ID PRJNA680496. Using Auxin-inducible-degradation System to Interrogate Tissue-specific Transcriptional Programs of HSF-1 in Reproduction and Heat Shock Response.

References

1. Costa, D.L., Yetter, N., and Desomer, H. (2018). Intergenerational transmission of paternal trauma among US Civil War ex-POWs. Proc. Natl. Acad. Sci. U. S. A. *115*, 11215–11220. https://doi.org/10.1073/PNAS.1803630115/SUPPL_FILE/PNAS.1803630115.SAPP.PDF.

2. Bohacek, J., Gapp, K., Saab, B.J., and Mansuy, I.M. (2013). Transgenerational Epigenetic Effects on Brain Functions. Biol. Psychiatry *73*, 313–320. https://doi.org/10.1016/J.BIOPSYCH.2012.08.019.

3. Nilsson, E.E., Sadler-Riggleman, I., and Skinner, M.K. (2018). Environmentally induced epigenetic transgenerational inheritance of disease. Environ. Epigenetics *4*, dvy016. https://doi.org/10.1093/eep/dvy016.

4. Beltran, T., Shahrezaei, V., Katju, V., and Sarkies, P. (2020). Epimutations driven by small RNAs arise frequently but most have limited duration in Caenorhabditis elegans. Nat. Ecol. Evol. *4*, 1539–1548. https://doi.org/10.1038/S41559-020-01293-Z.

5. Witvliet, D., Mulcahy, B., Mitchell, J.K., Meirovitch, Y., Berger, D.R., Wu, Y., Liu, Y., Koh, W.X., Parvathala, R., Holmyard, D., et al. (2021). Connectomes across development reveal principles of brain maturation. Nat. 2021 5967871 *596*, 257–261. https://doi.org/10.1038/s41586-021-03778-8.

6. Cook, S.J., Jarrell, T.A., Brittin, C.A., Wang, Y., Bloniarz, A.E., Yakovlev, M.A., Nguyen, K.C.Q., Tang, L.T.H., Bayer, E.A., Duerr, J.S., et al. (2019). Whole-animal connectomes of

both Caenorhabditis elegans sexes. Nat. 2019 5717763 *571*, 63–71. https://doi.org/10.1038/s41586-019-1352-7.

7. Brittin, C.A., Cook, S.J., Hall, D.H., Emmons, S.W., and Cohen, N. (2021). A multi-scale brain map derived from whole-brain volumetric reconstructions. Nature *591*, 105–110. https://doi.org/10.1038/S41586-021-03284-X.

8. Graham White, J., Southgate, E., Thomson, J.N., and Sydney, B. (1986). The structure of the nervous system of the nematode Caenorhabditis elegans. Philos. Trans. R. Soc. London. B, Biol. Sci. *314*, 1–340. https://doi.org/10.1098/rstb.1986.0056.

9. Ketting, R.F., and Cochella, L. (2021). Concepts and functions of small RNA pathways in C. elegans. Curr. Top. Dev. Biol. *144*, 45–89. https://doi.org/10.1016/BS.CTDB.2020.08.002.

10. Frolows, N., and Ashe, A. (2021). Small RNAs and chromatin in the multigenerational epigenetic landscape of Caenorhabditis elegans. Philos. Trans. R. Soc. B *376*. https://doi.org/10.1098/RSTB.2020.0112.

11. Timmons, L., Court, D.L., and Fire, A. (2001). Ingestion of bacterially expressed dsRNAs can produce specific and potent genetic interference in Caenorhabditis elegans. Gene *263*, 103–112. https://doi.org/10.1016/S0378-1119(00)00579-5.

12. Alcazar, R.M., Lin, R., and Fire, A.Z. (2008). Transmission dynamics of heritable silencing induced by double-stranded RNA in Caenorhabditis elegans. Genetics *180*, 1275–1288. https://doi.org/10.1534/genetics.108.089433.

13. Rechavi, O., Minevich, G., and Hobert, O. (2011). Transgenerational inheritance of an

acquired small RNA-based antiviral response in C. elegans. Cell *147*, 1248–1256. https://doi.org/10.1016/j.cell.2011.10.042.

14. Aoki, K., Moriguchi, H., Yoshioka, T., Okawa, K., and Tabara, H. (2007). In vitro analyses of the production and activity of secondary small interfering RNAs in C. elegans. EMBO J. *26*, 5007–5019. https://doi.org/10.1038/.

15. Sapetschnig, A., Sarkies, P., Lehrbach, N.J., and Miska, E.A. (2015). Tertiary siRNAs mediate paramutation in C. elegans. PLoS Genet. *11*, e1005078. https://doi.org/10.1371/journal.pgen.1005078.

16. Pak, J., and Fire, A. (2007). Distinct populations of primary and secondary effectors during RNAi in C. elegans. Science (80-.). *315*, 241–244. https://doi.org/10.1126/SCIENCE.1132839/SUPPL_FILE/PAK.SOM.PDF.

17. Shukla, A., Yan, J., Pagano, D.J., Dodson, A.E., Fei, Y., Gorham, J., Seidman, J.G., Wickens, M., and Kennedy, S. (2020). poly(UG)-tailed RNAs in genome protection and epigenetic inheritance. Nat. 2020 5827811 *582*, 283–288. https://doi.org/10.1038/s41586-020-2323-8.

18. Ouyang, J.P.T., Zhang, W.L., and Seydoux, G. (2022). The conserved helicase ZNFX-1 memorializes silenced RNAs in perinuclear condensates. Nat. Cell Biol. 2022 247 *24*, 1129–1140. https://doi.org/10.1038/s41556-022-00940-w.

19. Devanapally, S., Ravikumar, S., and Jose, A.M. (2015). Double-stranded RNA made in C. Elegans neurons can enter the germline and cause transgenerational gene silencing.

Proc. Natl. Acad. Sci. U. S. A. *112*, 2133–2138.

20. Joyce, P.I., Gallagher, J.M., and Kuwabara, P.E. (2006). Manipulating and enhancing the RNAi response.

21. Posner, R., Toker, I.A., Antonova, O., Bracha, S., Gingold, H., and Correspondence, O.R. (2019). Neuronal Small RNAs Control Behavior Transgenerationally. Cell *177*, 1814-1826.e15. https://doi.org/10.1016/j.cell.2019.04.029.

22. Fire, A., Xu, S., Montgomery, M.K., Kostas, S.A., Driver, S.E., and Mello, C.C. (1998). Potent and specific genetic interference by double-stranded RNA in Caenorhabditis elegans. Nature *391*, 806–811. https://doi.org/10.1038/35888.

23. Winston, W.M., Molodowitch, C., and Hunter, C.P. (2002). Systemic RNAi in C. elegans requires the putative transmembrane protein SID-1. Science (80-.). *295*, 2456–2459. https://doi.org/10.1126/SCIENCE.1068836/SUPPL_FILE/1068836S4_THUMB.GIF.

24. Houri-Ze'evi, L., Korem, Y., Sheftel, H., Faigenbloom, L., Toker, I.A., Dagan, Y., Awad, L., Degani, L., Alon, U., and Rechavi, O. (2016). A Tunable Mechanism Determines the Duration of the Transgenerational Small RNA Inheritance in C. elegans. Cell *165*, 88–99. https://doi.org/10.1016/j.cell.2016.02.057.

25. Houri-Zeevi, L., Korem Kohanim, Y., Antonova, O., and Rechavi, O. (2020). Three Rules Explain Transgenerational Small RNA Inheritance in C. elegans. Cell *182*, 1186-1197.e12. https://doi.org/10.1016/j.cell.2020.07.022.

26. Buckley, B.A., Burkhart, K.B., Gu, S.G., Spracklin, G., Kershner, A., Fritz, H., Kimble, J., Fire,

A., and Kennedy, S. (2012). A nuclear Argonaute promotes multigenerational epigenetic inheritance and germline immortality. Nature *489*, 447–451. https://doi.org/10.1038/nature11352.

27. Lev, I., Seroussi, U., Gingold, H., Bril, R., Anava, S., and Rechavi, O. (2017). MET-2-Dependent H3K9 Methylation Suppresses Transgenerational Small RNA Inheritance. Curr. Biol. *27*, 1138–1147. https://doi.org/10.1016/j.cub.2017.03.008.

28. Spracklin, G., Fields, B., Wan, G., Becker, D., Wallig, A., Shukla, A., and Kennedy, S. (2017). The RNAi inheritance machinery of caenorhabditis elegans. Genetics *206*, 1403–1416. https://doi.org/10.1534/genetics.116.198812.

29. Ouyang, J.P.T., Folkmann, A., Bernard, L., Lee, C.Y., Seroussi, U., Charlesworth, A.G., Claycomb, J.M., and Seydoux, G. (2019). P Granules Protect RNA Interference Genes from Silencing by piRNAs. Dev. Cell *50*, 716-728.e6. https://doi.org/10.1016/j.devcel.2019.07.026.

30. Seroussi, U., Lugowski, A., Wadi, L., Lao, R.X., Willis, A.R., Zhao, W., Sundby, A.E., Charlesworth, A.G., Reinke, A.W., and Claycomb, J.M. (2023). A comprehensive survey of c. Elegans argonaute proteins reveals organismwide gene regulatory networks and functions. Elife *12*. https://doi.org/10.7554/ELIFE.83853.

31. Yang, H., Zhang, Y., Vallandingham, J., Li, H., Florens, L., and Mak, H.Y. (2012). The RDE-10/RDE-11 complex triggers RNAi-induced mRNA degradation by association with target mRNA in C. elegans. Genes Dev. https://doi.org/10.1101/gad.180679.111.

32. Luteijn, M.J., Van Bergeijk, P., Kaaij, L.J.T., Almeida, M.V., Roovers, E.F., Berezikov, E., and Ketting, R.F. (2012). Extremely stable Piwi-induced gene silencing in Caenorhabditis elegans. EMBO J. *31*, 3422–3430. https://doi.org/10.1038/EMBOJ.2012.213/SUPPL_FILE/EMBJ2012213.REVIEWER_COMMENTS.PDF.

33. Shirayama, M., Seth, M., Lee, H.-C., Gu, W., Ishidate, T., Conte, D., and Mello, C.C. (2012). piRNAs initiate an epigenetic memory of nonself RNA in the C. elegans germline. Cell *150*, 65–77. https://doi.org/10.1016/j.cell.2012.06.015.

34. Ashe, A., Sapetschnig, A., Weick, E.-M.M., Mitchell, J., Bagijn, M.P., Cording, A.C., Doebley, A.-L.L., Goldstein, L.D., Lehrbach, N.J., Le Pen, J., et al. (2012). piRNAs can trigger a multigenerational epigenetic memory in the germline of C. elegans. Cell *150*, 88–99. https://doi.org/10.1016/j.cell.2012.06.018.

35. Gammon, D.B., Ishidate, T., Li, L., Gu, W., Silverman, N., and Mello, C.C. (2017). The Antiviral RNA Interference Response Provides Resistance to Lethal Arbovirus Infection and Vertical Transmission in Caenorhabditis elegans. Curr. Biol. *27*, 795–806. https://doi.org/10.1016/j.cub.2017.02.004.

36. Kaletsky, R., Moore, R.S., Vrla, G.D., Parsons, L.R., Gitai, Z., and Murphy, C.T. (2020). C. elegans interprets bacterial non-coding RNAs to learn pathogenic avoidance. Nature *586*, 445–451. https://doi.org/10.1038/s41586-020-2699-5.

37. Rechavi, O., Houri-Ze'evi, L., Anava, S., Goh, W.S.S., Kerk, S.Y., Hannon, G.J., and Hobert, O. (2014). Starvation-Induced Transgenerational Inheritance of Small RNAs in C. elegans.

Cell *158*, 277–287. https://doi.org/10.1016/j.cell.2014.06.020.

38. Jobson, M.A., Jordan, J.M., Sandrof, M.A., Hibshman, J.D., Lennox, A.L., and Baugh, L.R. (2015). Transgenerational effects of early life starvation on growth, reproduction, and stress resistance in Caenorhabditis elegans. Genetics. https://doi.org/10.1534/genetics.115.178699.

39. Kishimoto, S., Uno, M., Okabe, E., Nono, M., Nishida, E., Gaydos, L.J., Wang, W., Strome, S., Seong, K.H., Li, D., et al. (2017). Environmental stresses induce transgenerationally inheritable survival advantages via germline-to-soma communication in Caenorhabditis elegans. Nat. Commun. *8*, 14031. https://doi.org/10.1038/ncomms14031.

40. Vogt, M.C., and Hobert, O. (2023). Starvation-induced changes in somatic insulin/IGF-1R signaling drive metabolic programming across generations. Sci. Adv. *9*. https://doi.org/10.1126/SCIADV.ADE1817/SUPPL_FILE/SCIADV.ADE1817_DATA_S1_TO_S12.ZIP.

41. Rodgers, A.B., Morgan, C.P., Leu, N.A., and Bale, T.L. (2015). Transgenerational epigenetic programming via sperm microRNA recapitulates effects of paternal stress. Proc. Natl. Acad. Sci. *112*, 13699–13704. https://doi.org/10.1073/pnas.1508347112.

42. Schott, D., Yanai, I., and Hunter, C.P. (2014). Natural RNA interference directs a heritable response to the environment. Sci. Rep. *4*, 1–10. https://doi.org/10.1038/srep07387.

43. Klosin, A., Casas, E., Hidalgo-Carcedo, C., Vavouri, T., and Lehner, B. (2017). Transgenerational transmission of environmental information in C. elegans. Science (80-.

). *356*, 320–323. https://doi.org/10.1126/science.aah6412.

44. Belicard, T., Jareosettasin, P., and Sarkies, P. (2018). The piRNA pathway responds to environmental signals to establish intergenerational adaptation to stress. BMC Biol. *16*, 103. https://doi.org/10.1186/s12915-018-0571-y.

45. Zhang, D., Tu, S., Stubna, M., Wu, W.S., Huang, W.C., Weng, Z., and Lee, H.C. (2018). The piRNA targeting rules and the resistance to piRNA silencing in endogenous genes. Science (80-.). *359*, 587–592. https://doi.org/10.1126/science.aao2840.

46. Kimura, K.D., Miyawaki, A., Matsumoto, K., and Mori, I. (2004). The C. elegans thermosensory neuron AFD responds to warming. Curr. Biol. *14*, 1291–1295. https://doi.org/10.1016/j.cub.2004.06.060.

47. Goodman, M.B., and Sengupta, P. (2018). The extraordinary AFD thermosensor of C. elegans at Springer Verlag, https://doi.org/10.1007/s00424-017-2089-5 https://doi.org/10.1007/s00424-017-2089-5.

48. Hawk, J.D., Calvo, A.C., Liu, P., Wang, Z.-W., Samuel, A.D.T., Coló, D.A., Correspondence, -Ramos, Almoril-Porras, A., Aljobeh, A., Torruella-Suá Rez, M.L., et al. (2018). Integration of Plasticity Mechanisms within a Single Sensory Neuron of C. elegans Actuates a Memory Article Integration of Plasticity Mechanisms within a Single Sensory Neuron of C. elegans Actuates a Memory. https://doi.org/10.1016/j.neuron.2017.12.027.

49. Goodman, M.B., and Sengupta, P. (2019). How caenorhabditis elegans senses mechanical stress, temperature, and other physical stimuli. Genetics *212*, 25–51.

https://doi.org/10.1534/genetics.118.300241.

50. Kotera, I., Tran, N.A., Fu, D., Kim, J.H.J., Byrne Rodgers, J., and Ryu, W.S. (2016). Pan-neuronal screening in Caenorhabditis elegans reveals asymmetric dynamics of AWC neurons is critical for thermal avoidance behavior. Elife *5*. https://doi.org/10.7554/eLife.19021.

51. Ohta, A., Ujisawa, T., Sonoda, S., and Kuhara, A. (2014). Light and pheromone-sensing neurons regulates cold habituation through insulin signalling in Caenorhabditis elegans. Nat. Commun. *5*. https://doi.org/10.1038/ncomms5412.

52. Mori, I., and Ohshima, Y. (1995). Neural regulation of thermotaxis in Caenorhabditis elegans. Nature *376*, 344–348. https://doi.org/10.1038/376344a0.

53. Luo, L., Clark, D.A., Biron, D., Mahadevan, L., and Samuel, A.D.T. (2006). Sensorimotor control during isothermal tracking in Caenorhabditis elegans. J. Exp. Biol. *209*, 4652–4662. https://doi.org/10.1242/jeb.02590.

54. Ramot, D., MacInnis, B.L., and Goodman, M.B. (2008). Bidirectional temperature-sensing by a single thermosensory neuron in C. elegans. Nat. Neurosci. *11*, 908–915. https://doi.org/10.1038/nn.2157.

55. Ippolito, D., Thapliyal, S., and Glauser, D.A. (2021). Ca2+ /CaM binding to CaMKI promotes ima-3 importin binding and nuclear translocation in sensory neurons to control behavioral adaptation. Elife *10*. https://doi.org/10.7554/ELIFE.71443.

56. Prahlad, V., Cornelius, T., and Morimoto, R.I. (2008). Regulation of the cellular heat shock

response in Caenorhabditis elegans by thermosensory neurons. Science (80-.). *320*, 811–814. https://doi.org/10.1126/science.1156093.

57. Tatum, M.C., Ooi, F.K., Chikka, M.R., Chauve, L., Martinez-Velazquez, L.A., Steinbusch, H.W.M.M., Morimoto, R.I., and Prahlad, V. (2015). Neuronal Serotonin Release Triggers the Heat Shock Response in C. elegans in the Absence of Temperature Increase. Curr. Biol. *25*, 163–174. https://doi.org/10.1016/j.cub.2014.11.040.

58. Chen, Y.C., Chen, H.J., Tseng, W.C., Hsu, J.M., Huang, T.T., Chen, C.H., and Pan, C.L. (2016). A C. elegans Thermosensory Circuit Regulates Longevity through crh-1/CREB-Dependent flp-6 Neuropeptide Signaling. Dev. Cell *39*, 209–223. https://doi.org/10.1016/j.devcel.2016.08.021.

59. Sugi, T., Nishida, Y., and Mori, I. (2011). Regulation of behavioral plasticity by systemic temperature signaling in Caenorhabditis elegans. Nat. Neurosci. 2011 148 *14*, 984–992. https://doi.org/10.1038/nn.2854.

60. Servello, F.A., Fernandes, R., Eder, M., Harris, N., Martin, O.M.F., Oswal, N., Lindberg, A., Derosiers, N., Sengupta, P., Stroustrup, N., et al. (2022). Neuronal temperature perception induces specific defenses that enable C. elegans to cope with the enhanced reactivity of hydrogen peroxide at high temperature. Elife *11*. https://doi.org/10.7554/ELIFE.78941.

61. Deshe, N., Eliezer, Y., Hoch, L., Itskovits, E., Bokman, E., Ben-Ezra, S., and Zaslaver, A. (2023). Inheritance of associative memories and acquired cellular changes in C. elegans. Nat. Commun. 2023 141 *14*, 1–15. https://doi.org/10.1038/s41467-023-39804-8.

62. Perez, M.F., Shamalnasab, M., Mata-Cabana, A., Della Valle, S., Olmedo, M., Francesconi, M., and Lehner, B. (2021). Neuronal perception of the social environment generates an inherited memory that controls the development and generation time of C. elegans. Curr. Biol. *31*, 4256-4268.e7. https://doi.org/10.1016/j.cub.2021.07.031.

63. Baugh, L.R., and Day, T. (2020). Nongenetic inheritance and multigenerational plasticity in the Nematode C. elegans. Elife *9*, 1–13. https://doi.org/10.7554/ELIFE.58498.

64. Cheeks, R.J., Canman, J.C., Gabriel, W.N., Meyer, N., Strome, S., and Goldstein, B. (2004). C. elegans PAR Proteins Function by Mobilizing and Stabilizing Asymmetrically Localized Protein Complexes. Curr. Biol. *14*, 851–862. https://doi.org/10.1016/J.CUB.2004.05.022.

65. Praitis, V., Casey, E., Collar, D., and Austin, J. (2001). Creation of low-copy integrated transgenic lines in Caenorhabditis elegans. Genetics *157*, 1217–1226. https://doi.org/10.1093/GENETICS/157.3.1217.

66. Pokala, N., Liu, Q., Gordus, A., and Bargmann, C.I. (2014). Inducible and titratable silencing of Caenorhabditis elegans neurons in vivo with histamine-gated chloride channels. Proc. Natl. Acad. Sci. *111*, 2770 LP – 2775. https://doi.org/10.1073/pnas.1400615111.

67. Ikeda, M., Nakano, S., Giles, A.C., Xu, L., Costa, W.S., Gottschalk, A., and Mori, I. (2020). Context-dependent operation of neural circuits underlies a navigation behavior in Caenorhabditis elegans. Proc. Natl. Acad. Sci. U. S. A. *117*, 6178–6188. https://doi.org/10.1073/PNAS.1918528117/SUPPL_FILE/PNAS.1918528117.SM02.AVI.

68. Li, R., Xu, Y., Wen, X., Chen, Y.H., Wang, P.Z., Zhao, J.L., Wu, P.P., Wu, J.J., Liu, H., Huang, J.H., et al. (2024). GCY-20 signaling controls suppression of Caenorhabditis elegans egg laying by moderate cold. Cell Rep. *43*. https://doi.org/10.1016/J.CELREP.2024.113708/ATTACHMENT/F95ACB80-E442-482B-A9AD-B24BCBE455E9/MMC2.PDF.

69. Troemel, E.B., Chou, J.H., Dwyer, N.D., Colbert, H.A., and Bargmann Howard, C.I. (1995). Divergent Seven Transmembrane Receptors Are Candidate Chemosensory Receptors in C. elegans. Cell *83*, 207–218.

70. Takeishi, A., Yeon, J., Harris, N., Yang, W., and Sengupta, P. (2020). Feeding state functionally reconfigures a sensory circuit to drive thermosensory behavioral plasticity. Elife *9*, 1–25. https://doi.org/10.7554/ELIFE.61167.

71. Inada, H., Ito, H., Satterlee, J., Sengupta, P., Matsumoto, K., and Mori, I. (2006). Identification of Guanylyl Cyclases That Function in Thermosensory Neurons of Caenorhabditis elegans. Genetics *172*, 2239. https://doi.org/10.1534/GENETICS.105.050013.

72. Wasserman, S.M., Beverly, M., Bell, H.W., and Sengupta, P. (2011). Regulation of response properties and operating range of the AFD thermosensory neurons by cGMP signaling. Curr. Biol. *21*, 353–362. https://doi.org/10.1016/j.cub.2011.01.053.

73. Takeishi, A., Yu, Y. V., Hapiak, V.M., Bell, H.W., O'Leary, T., and Sengupta, P. (2016). Receptor-type Guanylyl Cyclases Confer Thermosensory Responses in C. elegans. Neuron *90*, 235–244. https://doi.org/10.1016/j.neuron.2016.03.002.

74. Yu, S., Avery, L., Baude, E., and Garbers, D.L. (1997). Guanylyl cyclase expression in specific sensory neurons: A new family of chemosensory receptors. Proc. Natl. Acad. Sci. U. S. A. *94*, 3384–3387. https://doi.org/10.1073/pnas.94.7.3384.

75. Kagoshima, H., and Kohara, Y. (2015). Co-expression of the transcription factors CEH-14 and TTX-1 regulates AFD neuron-specific genes gcy-8 and gcy-18 in C. elegans. Dev. Biol. *399*, 325–336. https://doi.org/10.1016/J.YDBIO.2015.01.010.

76. Taylor, S.R., Santpere, G., Weinreb, A., Barrett, A., Reilly, M.B., Xu, C., Varol, E., Oikonomou, P., Glenwinkel, L., McWhirter, R., et al. (2021). Molecular topography of an entire nervous system. Cell *184*, 4329-4347.e23. https://doi.org/10.1016/J.CELL.2021.06.023.

77. Satterlee, J.S., Ryu, W.S., and Sengupta, P. (2004). The CMK-1 CaMKI and the TAX-4 Cyclic Nucleotide-Gated Channel Regulate Thermosensory Neuron Gene Expression and Function in C. elegans. Curr. Biol. *14*, 62–68. https://doi.org/10.1016/j.cub.2003.12.030.

78. Yu, Y. V., Bell, H.W., Glauser, D.A., VanHooser, S.D., Goodman, M.B., and Sengupta, P. (2014). CaMKI-dependent regulation of sensory gene expression mediates experience-dependent plasticity in the operating range of a thermosensory neuron. Neuron *84*, 919. https://doi.org/10.1016/J.NEURON.2014.10.046.

79. Kimura, Y., Corcoran, E.E., Eto, K., Gengyo-Ando, K., Muramatsu, M.A., Kobayashi, R., Freedman, J.H., Mitani, S., Hagiwara, M., Means, A.R., et al. (2002). A CaMK cascade activates CRE-mediated transcription in neurons of Caenorhabditis elegans. EMBO Rep. *3*, 962–966. https://doi.org/10.1093/EMBO-REPORTS/KVF191.

80. Harris, N., Bates, S.G., Zhuang, Z., Bernstein, M., Stonemetz, J.M., Hill, T.J., Yu, Y. V., Calarco, J.A., and Sengupta, P. (2023). Molecular encoding of stimulus features in a single sensory neuron type enables neuronal and behavioral plasticity. Curr. Biol. *33*, 1487-1501.e7. https://doi.org/10.1016/j.cub.2023.02.073.

81. Hajdu-Cronin, Y.M., Chen, W.J., and Sternberg, P.W. (2004). The L-Type Cyclin CYL-1 and the Heat-Shock-Factor HSF-1 Are Required for Heat-Shock-Induced Protein Expression in Caenorhabditis elegans. Genetics *168*, 1937. https://doi.org/10.1534/GENETICS.104.028423.

82. Maeda, I., Kohara, Y., Yamamoto, M., and Sugimoto, A. (2001). Large-scale analysis of gene function in Caenorhabditis elegans by high-throughput RNAi. Curr. Biol. *11*, 171–176. https://doi.org/10.1016/S0960-9822(01)00052-5.

83. Simmer, F., Moorman, C., Van Der Linden, A.M., Kuijk, E., Van Den Berghe, P.V.E., Kamath, R.S., Fraser, A.G., Ahringer, J., and Plasterk, R.H.A. (2003). Genome-Wide RNAi of C. elegans Using the Hypersensitive rrf-3 Strain Reveals Novel Gene Functions. PLoS Biol. *1*. https://doi.org/10.1371/JOURNAL.PBIO.0000012.

84. Xu, F., Feng, X., Chen, X., Weng, C., Yan, Q., Xu, T., Hong, M., and Guang, S. (2018). A Cytoplasmic Argonaute Protein Promotes the Inheritance of RNAi. Cell Rep. *23*, 2482–2494.

85. Charlesworth, A.G., Seroussi, U., Lehrbach, N.J., Renaud, M.S., Sundby, A.E., Molnar, R.I., Lao, R.X., Willis, A.R., Woock, J.R., Aber, M.J., et al. (2021). Two isoforms of the essential C. elegans Argonaute CSR-1 differentially regulate sperm and oocyte fertility. Nucleic

Acids Res. *49*, 8836–8865. https://doi.org/10.1093/NAR/GKAB619.

86. Wan, G., Fields, B.D., Spracklin, G., Shukla, A., Phillips, C.M., and Kennedy, S. (2018). Spatiotemporal regulation of liquid-like condensates in epigenetic inheritance. Nature *557*, 679–683. https://doi.org/10.1038/s41586-018-0132-0.

87. Gerson-Gurwitz, A., Wang, S., Sathe, S., Green, R., Yeo, G.W., Oegema, K., and Desai, A. (2016). A Small RNA-Catalytic Argonaute Pathway Tunes Germline Transcript Levels to Ensure Embryonic Divisions. Cell. https://doi.org/10.1016/j.cell.2016.02.040.

88. Wedeles, C.J., Wu, M.Z., and Claycomb, J.M. (2013). A multitasking Argonaute: Exploring the many facets of C. elegans CSR-1. Chromosom. Res. *21*, 573–586. https://doi.org/10.1007/S10577-013-9383-7/METRICS.

89. Quarato, P., Singh, M., Cornes, E., Li, B., Bourdon, L., Mueller, F., Didier, C., and Cecere, G. (2021). Germline inherited small RNAs facilitate the clearance of untranslated maternal mRNAs in C. elegans embryos. Nat. Commun. 2021 121 *12*, 1–14. https://doi.org/10.1038/s41467-021-21691-6.

90. Edwards, S.L., Erdenebat, P., Morphis, A.C., Kumar, L., Wang, L., Chamera, T., Georgescu, C., Wren, J.D., and Li, J. (2021). Insulin/IGF-1 signaling and heat stress differentially regulate HSF1 activities in germline development. Cell Rep. *36*, 109623. https://doi.org/10.1016/J.CELREP.2021.109623/ATTACHMENT/CC4AEBA7-7D2C-41A5-8468-C56D1E66EB19/MMC7.XLSX.

91. Jose, A.M. (2023). Heritable epigenetic changes are constrained by the dynamics of

regulatory architectures. Elife *12*. https://doi.org/10.7554/ELIFE.92093.1.

92. Karin, O., Miska, E.A., and Simons, B.D. (2023). Epigenetic inheritance of gene silencing is maintained by a self-tuning mechanism based on resource competition. Cell Syst. *14*, 24-40.e11. https://doi.org/10.1016/J.CELS.2022.12.003/ATTACHMENT/C938DF19-1283-40D2-A7A0-EB4B03439A50/MMC9.PDF.

93. Kim, K., and Li, C. (2004). Expression and regulation of an FMRFamide-related neuropeptide gene family in Caenorhabditis elegans. J. Comp. Neurol. *475*, 540–550. https://doi.org/10.1002/CNE.20189.

94. Li, J., Chauve, L., Phelps, G., Brielmann, R.M., and Morimoto, R.I. (2016). E2F coregulates an essential HSF developmental program that is distinct from the heat-shock response. Genes Dev. *30*, 2062–2075. https://doi.org/10.1101/GAD.283317.116/-/DC1.

95. Douglas, P.M., Baird, N.A., Simic, M.S., Uhlein, S., McCormick, M.A., Wolff, S.C., Kennedy, B.K., and Dillin, A. (2015). Heterotypic signals from neural HSF-1 separate thermotolerance from longevity. Cell Rep. *12*, 1196. https://doi.org/10.1016/J.CELREP.2015.07.026.

96. Gómez-Orte, E., Cornes, E., Zheleva, A., Sáenz-Narciso, B., de Toro, M., Iñiguez, M., López, R., San-Juan, J.F., Ezcurra, B., Sacristán, B., et al. (2018). Effect of the diet type and temperature on the C. elegans transcriptome. Oncotarget *9*, 9556. https://doi.org/10.18632/ONCOTARGET.23563.

97. Zhang, B., Xiao, R., Ronan, E.A., He, Y., Hsu, A.L., Liu, J., and Xu, X.Z.S. (2015).

Environmental temperature differentially modulates C. elegans longevity through a thermosensitive TRP channel. Cell Rep. *11*, 1414. https://doi.org/10.1016/J.CELREP.2015.04.066.

98. Petrella, L.N. (2014). Natural Variants of C. elegans Demonstrate Defects in Both Sperm Function and Oogenesis at Elevated Temperatures. PLoS One *9*, 112377. https://doi.org/10.1371/JOURNAL.PONE.0112377.

99. Houri-Zeevi, L., Teichman, G., Gingold, H., and Rechavi, O. (2021). Stress resets ancestral heritable small RNA responses. Elife *10*. https://doi.org/10.7554/eLife.65797.

100. Mallard, F., Nolte, V., and Schlötterer, C. (2020). The Evolution of Phenotypic Plasticity in Response to Temperature Stress. Genome Biol. Evol. *12*, 2429–2440. https://doi.org/10.1093/GBE/EVAA206.

101. Liu, L., Ruediger, C., and Shapira, M. (2018). Integration of Stress Signaling in Caenorhabditis elegans Through Cell-Nonautonomous Contributions of the JNK Homolog KGB-1. Genetics *210*, 1317–1328. https://doi.org/10.1534/genetics.118.301446.

102. Bishop, N.A., and Guarente, L. (2007). Two neurons mediate diet-restriction-induced longevity in C. elegans. Nature *447*, 545–549. https://doi.org/10.1038/nature05904.

103. Prahlad, V., and Morimoto, R.I. (2011). Neuronal circuitry regulates the response of Caenorhabditis elegans to misfolded proteins. Proc. Natl. Acad. Sci. U. S. A. *108*, 14204–14209. https://doi.org/10.1073/pnas.1106557108.

104. Fletcher, M., and Kim, D.H. (2017). Age-Dependent Neuroendocrine Signaling from

Sensory Neurons Modulates the Effect of Dietary Restriction on Longevity of Caenorhabditis elegans. PLoS Genet. *13*. https://doi.org/10.1371/journal.pgen.1006544.

105. Boulias, K., and Horvitz, H.R. (2012). The C. elegans MicroRNA mir-71 acts in neurons to promote germline-mediated longevity through regulation of DAF-16/FOXO. Cell Metab. *15*, 439–450. https://doi.org/10.1016/j.cmet.2012.02.014.

106. Teichman, G. (2023). DoubleBlind: Blind and unblind file names automatically to maintain experimental integrity. https://github.com/GuyTeichman/DoubleBlind.

107. Schindelin, J., Arganda-Carreras, I., Frise, E., Kaynig, V., Longair, M., Pietzsch, T., Preibisch, S., Rueden, C., Saalfeld, S., Schmid, B., et al. (2012). Fiji: an open-source platform for biological-image analysis. Nat. Methods *9*, 676–682. https://doi.org/10.1038/nmeth.2019.

108. Hammond, L. (University of Q. (2014). Measuring cell fluorescence using ImageJ — The Open Lab Book v1.0. https://theolb.readthedocs.io/en/latest/imaging/measuring-cell-fluorescence-using-imagej.html.

109. Benjamini, Y., Krieger, A.M., and Yekutieli, D. (2006). Adaptive linear step-up procedures that control the false discovery rate. Biometrika *93*, 491–507.

110. Teichman, G., Cohen, D., Ganon, O., Dunsky, N., Shani, S., Gingold, H., and Rechavi, O. (2023). RNAlysis: analyze your RNA sequencing data without writing a single line of code. BMC Biol. *21*, 74. https://doi.org/10.1186/s12915-023-01574-6.

111. Andrews, S. (2010). FastQC A Quality Control tool for High Throughput Sequence Data.

http://www.bioinformatics.babraham.ac.uk/projects/fastqc/.

112. Martin, M. (2011). Cutadapt removes adapter sequences from high-throughput sequencing reads. EMBnet.journal *17*, 10–12. https://doi.org/10.14806/EJ.17.1.200.

113. Shahid, S., and Axtell, M.J. (2014). Identification and annotation of small RNA genes using ShortStack. Methods *67*, 20–27. https://doi.org/10.1016/j.ymeth.2013.10.004.

114. Liao, Y., Smyth, G.K., and Shi, W. (2014). featureCounts: an efficient general purpose program for assigning sequence reads to genomic features. Bioinformatics *30*, 923–930. https://doi.org/10.1093/BIOINFORMATICS/BTT656.

115. Kim, D., Paggi, J.M., Park, C., Bennett, C., and Salzberg, S.L. (2019). Graph-based genome alignment and genotyping with HISAT2 and HISAT-genotype. Nat. Biotechnol. *37*, 907–915. https://doi.org/10.1038/s41587-019-0201-4.

Figure Legends

Figure 1: The AFD thermosensory neurons control temperature-dependent small RNA-mediated gene silencing

(A) Representative images of worms containing the *bnIs1* transgene, grown in either high (25°C) or low (20°C) temperatures.

(B, C) The archetypal dynamics of transgene silencing and de-silencing upon transition between temperatures.

(D) Hyperpolarization of the AFD neurons suppresses transgene silencing upon transition to a low temperature.

(E) Knocking out AFD-specific guanylyl cyclases *gcy-8/18/23* inhibits transgene silencing upon transition to a low temperature.

Graphs B-E indicate the percentages of worms positive for GFP expression (Y-axis) in each generation (X-axis) and experimental condition (mean ± SEM). (*) indicates $q < 0.05$, (**) indicates $q < 0.01$, (***) indicates $q < 0.001$, and (****) indicates $q < 0.0001$ (see **Methods**).

Figure 2: A thermosensory circuit and HSF-1 regulates temperature-dependent transgenerational gene silencing

(A) A scheme of the AFD thermosensory circuit and its downstream components. Based on previous studies [47,55,57,58,78].

(B) – (D) Knockout of components in the AFD thermosensory circuit inhibits transgene silencing upon transition to a low temperature.

(E) Knocking out *hsf-1* inhibits transgene silencing upon transition to a low temperature.

(F) – (I) Knocking out of components in the AFD thermosensory circuit, with the exception of *cmk-1* (G), does not abolish the archetypal transgene de-silencing upon transition to a high temperature.

Graphs B-I indicate the percentages of worms positive for GFP expression (Y-axis) in each generation (X-axis) and experimental condition (mean ± SEM). (*) indicates $q < 0.05$, (**) indicates $q < 0.01$, (***) indicates $q < 0.001$, and (****) indicates $q < 0.0001$ (see **Methods**).

Figure 3: Identifying groups of endogenous small RNAs that accumulate transgenerationally in a sensation-dependent manner

(A) GFP expression data in wild-type worms and AFD triple mutants selected for small RNA sequencing (see **Methods** for the unbiased selection strategy). The graphs indicate the percentages of worms positive for GFP expression for each generation and experimental condition (mean ± SEM).

(B) Anti-*gfp* small RNAs accumulate transgenerationally in low temperatures in a sensation-dependent manner. Shown are Relative Log Expression-normalized anti-*gfp* small RNA levels (mean ± SEM). Each dot represents a biological replicate.

(C) Two groups of siRNAs exhibit different dynamics of transgenerational accumulation in AFD triple mutants and wild type upon transition from 25°C to 20°C. $\log_2$(FC) was calculated on normalized read counts that were averaged over biological replicates.

(D) Rate of endogenous small RNA accumulation is lower in AFD triple mutants compared to wild type. Shown are the standardized expression levels of the genes in each group over generations and conditions. Each line represents the standardized expression of a single siRNA, after being normalized and averaged over biological replicates. Bold lines represent the mean of all genes in that group. Left and right panels correspond to the left and right panels of (C) respectively.

(E) Fold enrichment and depletion for small RNAs (from C & D) based on their association with specific WAGOs. Left and right panels correspond to the left and right panels of (C) and (D) respectively.

(*) indicates $q < 0.05$, (**) indicates $q < 0.01$, (***) indicates $q < 0.001$, and (****) indicates $q < 0.0001$ (see **Methods**).

Figure 4: Temperature perception regulates endogenous small RNA pathways

(A) Experimental scheme. We sequenced mRNA and small RNAs from wild-type and *cmk-1* mutant worms across generations and temperatures. We grew worms at 20°C for multiple generations and then transferred them to 25°C for three generations. We established independent lineages from P0, tracking GFP expression throughout. We sequenced worms at P0 (20°C) and F3 (after three generations at 25°C). For F3 *cmk-1* mutants, we selected "expressing" (highest GFP expression) and "silencing" (lowest GFP expression) lineages, based on their F2 phenotypes. This allows comparison of differential responses to temperature change.

(B) Anti-*gfp* small RNA levels are downregulated upon transition to 25°C in a perception-dependent manner. Shown are $\log_2$(normalized read counts) of the small RNAs that target (antisense) the *bnIs1* transgene (Y-axis) against coordinates along the *bnIs1* transgene (X-axis) in wild-type worms and *cmk-1* mutants (expressing/silencing lineages) before (left) and after (right) transition to 25°C. Reads were normalized using the Relative Log Expression method.

(C) Anti-*gfp* small RNAs are downregulated upon transition to 25°C in a perception-dependent manner. Shown are Relative Log Expression-normalized read counts of the small RNAs that target the *bnIs1* transgene (antisense) under the different experimental conditions (mean ± SEM).

(D) Growing at 25°C and mutation in *cmk-1* downregulates small RNAs targeting protein-coding genes. Shown are the percentage of the total small RNA pool aligned to

different types of genomic features (mean ± SEM). Each dot depicts a biological replicate.

(E) piRNAs are downregulated at 25°C in wild-type worms but are upregulated at high temperatures in *cmk-1(oy21)* mutants. Shown are the $\log_2$(FC) values (mean ± SEM) of individual piRNAs in comparison to wild-type worms at 20°C.

(F) Growth at 25°C induces changes in small RNA pools in both a sensation-dependent and -independent manner. Shown are Venn diagrams of the siRNAs significantly up- or down-regulated in 25°C in wild-type worms only (green), *cmk-1(oy21)* mutants only (grey), or both (yellow).

(G) Sensation-dependent changes in siRNAs following temperature transition are enriched for specific Argonaute targets. Shown are fold enrichment and depletion values for downregulated (bottom) or upregulated siRNAs (top), and siRNAs that change in a sensation-dependent (right half) or -independent manner (left half). Roman numerals (I-IV) correspond to (F).

(*) indicates $q < 0.05$, (**) indicates $q < 0.01$, (***) indicates $q < 0.001$, and (****) indicates $q < 0.0001$ (see **Methods**).

Figure 5: The perception of low temperatures promotes the expression of small RNA machinery

(A) The expression of small RNA factors is increased in worms grown in 20°C (Y-axis) compared to worms grown in 25°C (X-axis). Shown are the averaged expression values (log_{1010} of Relative Log Expression-normalized read counts) of genes. Each dot represents a protein-coding gene. Orange dots represent epigenetic-related genes. Dotted line represents the diagonal (where expression values equal between the two conditions).

(B) The expression of small RNA factors is increased in wild-type worms (Y-axis) compared to *cmk-1(oy21)* mutants (X-axis).

(C) The expression of small RNA factors is reduced following AFD ablation. Shown is a Venn diagram depicting the sets of (1) genes downregulated following AFD ablation [60], (2) genes downregulated in *cmk-1(oy21)* mutants, (3) epigenetic genes. See **Methods** for details about differential expression analysis.

(D) The expression of small RNA factors is decreased upon germline-specific degradation of HSF-1. Shown are the Relative Log Expression-normalized expression levels (geometric mean ± GSEM) of two germline-specific Argonaute genes (*hrde-1* and *wago-1*) and two ubiquitous Argonautes (*ergo-1* and *nrde-3*). Each dot corresponds to a single biological replicate.

Figure 6: Predicting transgenerational small RNA-mediated gene silencing based on temperature perception

(A) The scheme and added assumptions of the expanded mathematical model describing the impacts of temperature perception on transgenerational small RNA inheritance. The basic model was previously described [92].

(B) The simulated dynamics of transgene silencing after transition from high to low temperatures, in wild-type worms (green) and temperature perception mutants (grey). Simulates the experiments presented in **Figure 2B-D**.

(C) The simulated dynamics of transgene de-silencing after transition from low to high temperatures in wild-type worms (green) and temperature perception mutants (grey). Simulates the experiments presented in **Figure 2F, H, I**.

(D) The simulated dynamics of transgene de-silencing after transition from low to high temperatures in wild-type worms (green) and *cmk-1(oy21)* mutants (grey). Simulates the experiment presented in **Figure 2G**.

The graphs indicate the mean percentages of worms positive for GFP expression for each generation and experimental condition (number of simulations = 1000).

Figure 7: Modified temperature perception, even in the absence of temperature change, repressed heritable small RNA responses

(A) The simulated dynamics of RNAi inheritance in wild-type worms (green) and temperature perception mutants (grey).

(B) Defective temperature perception, on its own, is sufficient to dampen transgenerational inheritance of RNAi responses initiated by exogenous dsRNA. The graph indicates the percentages of wild-type and *cmk-1(oy21)* worms positive for *mex-5::GFP* expression for each generation following initial RNAi treatment (mean ± SEM). (*) indicates $q < 0.05$, (**) indicates $q < 0.01$, (***) indicates $q < 0.001$, and (****) indicates $q < 0.0001$ (see **Methods**).

(C) A model summarizing our findings that temperature perception drives transgenerational small RNA inheritance. AFD-mediated temperature perception induces a cell-nonautonomous signaling cascade composed of GCY-8/18/23, CMK-1, FLP-6, and serotonin (5-HT) signaling. This cascade may modify the activity of the transcription factor HSF-1, which regulates the expression of small RNA machinery in the germline, facilitating changes in transgenerational small RNA inheritance.

Supplementary Figure 1: HRDE-1-dependent heritable small RNAs mediate Temperature-dependent silencing of GFP transgene

hrde-1(tm1200) mutants de-silence the *bnIs1* transgene even when grown at 20°C. The graph indicates the percentages of worms positive for GFP expression for each experimental condition (mean ± SEM). Each dot represents a biological replicate of the experiment that consists of at least 30 worms (see **Methods**).

Supplementary Figure 2: AFD-ablated worms exhibit delayed transgene silencing when transitioning from high to low temperature.

Worms carrying transgene expressing caspase in the AFD neurons exhibit delayed transgene silencing in the germline. The graph indicates the percentages of worms positive for GFP expression for each generation and experimental condition (mean ± SEM). (*) indicates $q < 0.05$, (**) indicates $q < 0.01$.

Supplementary Figure 3: HisCl1-mediated hyperpolarization abolishes temperature-dependent transgene silencing in an AFD-specific manner

(A) Histamine exposure reversibly hyperpolarizes HisCl1-expressing AFD neurons. Activity of the AFD sensory neurons was quantified by GCaMP6s fluorescence intensity in a microfluidic device controlling histamine exposure. Wild-type (n=14) and AFD:HisCl1 (n=14) worms were loaded into chips and exposed to 1mM HA for two periods of 20 seconds (20-40 seconds and 60-80 seconds, see yellow bars). Shown are the fluorescence intensity values over time, normalized to the initial fluorescence.

(B) Hyperpolarization of the AFD neurons suppresses transgene silencing upon transition to a low temperature, with the response lasting for at least 7 generations.

(C) Expression of HisCl1 and hyperpolarization of the ASK sensory neurons do not affect temperature-dependent transgene silencing.

The graphs in B-C indicate the percentages of worms positive for GFP expression for each generation and experimental condition (mean ± SEM). (*) indicates $q < 0.05$, (**) indicates $q < 0.01$, (***) indicates $q < 0.001$, and (****) indicates $q < 0.0001$ (see **Methods**).

Supplementary Figure 4: Single-copy expression of AFD:HisCl1 is not sufficient to abolish temperature-dependent transgene silencing

Single-copy expression of the histamine-gated chlorine channel HisCl1 under the *gcy-8* promoter does not suppress transgene silencing upon transition to a low temperature. The graph indicates the percentages of worms positive for GFP expression for each generation and experimental condition (mean ± SEM). (*) indicates $q < 0.05$, (**) indicates $q < 0.01$, (***) indicates $q < 0.001$, and (****) indicates $q < 0.0001$ (see **Methods**).

Supplementary Figure 5: AFD:HisCl1 +HA treatment has a dose-response effect

(A) Experimental scheme. AFD:HisCl1 and control worms were transitioned from a high to a low temperature. After each generation in the low temperature, some worms from the AFD:HisCl1+HA group were transitioned to plates no longer containing histamine, and were then tracked for more generations in those conditions. This led to the creation of five experimental groups, that were exposed to histamine for 5/4/3/2/1 generations in total.

(B) Histamine treatment of AFD:HisCl1 worms suppresses temperature-dependent silencing, even when the histamine treatment is stopped for 1-3 generations. The graph indicates the percentages of worms positive for GFP expression for each generation and experimental condition (mean ± SEM). (*) indicates $q < 0.05$, (**) indicates $q < 0.01$, (***) indicates $q < 0.001$, and (****) indicates $q < 0.0001$ (see **Methods**).

Supplementary Figure 6: AFD:HisCl1-induced changes in small RNA-mediated silencing last for at least 3 generations in the absence of AFD:HisCl1

(A) Experimental scheme. AFD:HisCl1 and control worms were transitioned from a high to a low temperature. After 4 generations in the low temperature, some worms from the AFD:HisCl1 group were selected to lose the extrachromosomal AFD:HisCl1 construct and were then tracked for three more generations in a low temperature.

(B) Worms whose ancestors expressed AFD:HisCl1 maintain GFP expression for at least 3 generations after losing the AFD:HisCl1 construct. The graph indicates the percentages of worms positive for GFP expression for each generation and experimental condition (mean ± SEM). (*) indicates $q < 0.05$, (**) indicates $q < 0.01$, (***) indicates $q < 0.001$, and (****) indicates $q < 0.0001$ (see **Methods**).

Supplementary Figure 7: A thermosensory circuit regulates temperature-dependent transgenerational silencing cell-nonautonomously through HSF-1 (individual trajectories)

(A) – (D) Knocking out components in the AFD thermosensory circuit inhibits transgene silencing upon transition to a low temperature.

(E) Knocking out *hsf-1* inhibits transgene silencing upon transition to a low temperature.

(F) – (I) Knocking out components in the AFD thermosensory circuit, with the exception of *cmk-1* (G), does not abolish the archetypal transgene de-silencing upon transition to a high temperature. We detected no effects except differences in baseline silencing levels at 20°C (i.e. no difference in the slope of their de-silencing response).

The graphs indicate the percentages of worms positive for GFP expression for each generation and experimental condition. Each line represents a replicate of the experiment, consisting of at least 30 worms per generation (see **Methods**).

Supplementary Figure 8: The long-term effects of the AFD thermosensory circuit on small RNA silencing

(A) The CaM Kinase gene *cmk-1* is expressed chiefly in the AFD neurons. Data is taken from the CeNGEN Project [76]. Shown is a scatter plot comparing the average TPM of *cmk-1* in various neuron classes (Y-axis) to the percentage of cells of various neuron classes with detectable expression of *cmk-1* (X-axis). Each dot represents a neuron class, with the orange dot representing the AFD neuron class.

(B) – (C) Knocking out the neuropeptide gene *flp-6* and the tryptophan hydroxylase gene *tph-1* inhibits temperature-dependent small RNA-mediated gene silencing for at least 10 generations following transition from high to low temperature. The graphs indicate the percentages of worms positive for GFP expression for each experimental condition (mean ± SEM). Each dot represents a replicate of the experiment that consists of at least 30 worms (see **Methods**).

Supplementary Figure 9: The serotonin receptor SER-1 is not involved in temperature-dependent transgene silencing

ser-1(ok345) mutants exhibit a typical silencing response upon transition from high to low temperature. The graph indicates the percentages of worms positive for GFP expression for each generation and experimental condition (mean ± SEM). (*) indicates $q < 0.05$, (**) indicates $q < 0.01$, (***) indicates $q < 0.001$, and (****) indicates $q < 0.0001$ (see **Methods**).

Supplementary Figure 10: Mutants of the CaM Kinase gene *cmk-1* exhibit a high-variance de-silencing response in high temperatures

When transitioned to high temperatures, *cmk-1(oy21)* mutants exhibit a high-variance de-silencing response, with some lineages completely de-silencing the GFP transgene, while others maintain complete silencing. Out of 27 replicates, we picked the three most extreme samples in each direction for RNA sequencing (see **Methods** for full experimental protocol).

The graph indicates the percentages of worms positive for GFP expression for each generation and experimental condition (mean ± SEM). Each dot represents a replicate (lineage) of the experiment that consists of at least 30 worms (see **Methods**).

Supplementary Figure 11: Modified temperature perception, even in the absence of temperature change, repressed heritable small RNA responses (individual trajectories)

(A) The basal expression level of the *mjIs134*[*mex-5p::gfp::h2b::tbb-2*] II transgene does not differ between wild-type worms and *cmk-1(oy21)* mutants. The graph indicates the Corrected Total Cell Fluorescence (CTCF) of each worm, relative to the average of wild-type worms (mean ± SEM). Each dot represents the average of three measurements of an individual worm (see **Methods**).

(B) Defective temperature perception, on its own, is sufficient to dampen transgenerational inheritance of RNAi responses. The graph indicates the percentages of worms positive for GFP expression for each generation and experimental condition. Each line represents a replicate of the experiment, consisting of at least 30 worms per generation (see **Methods**).

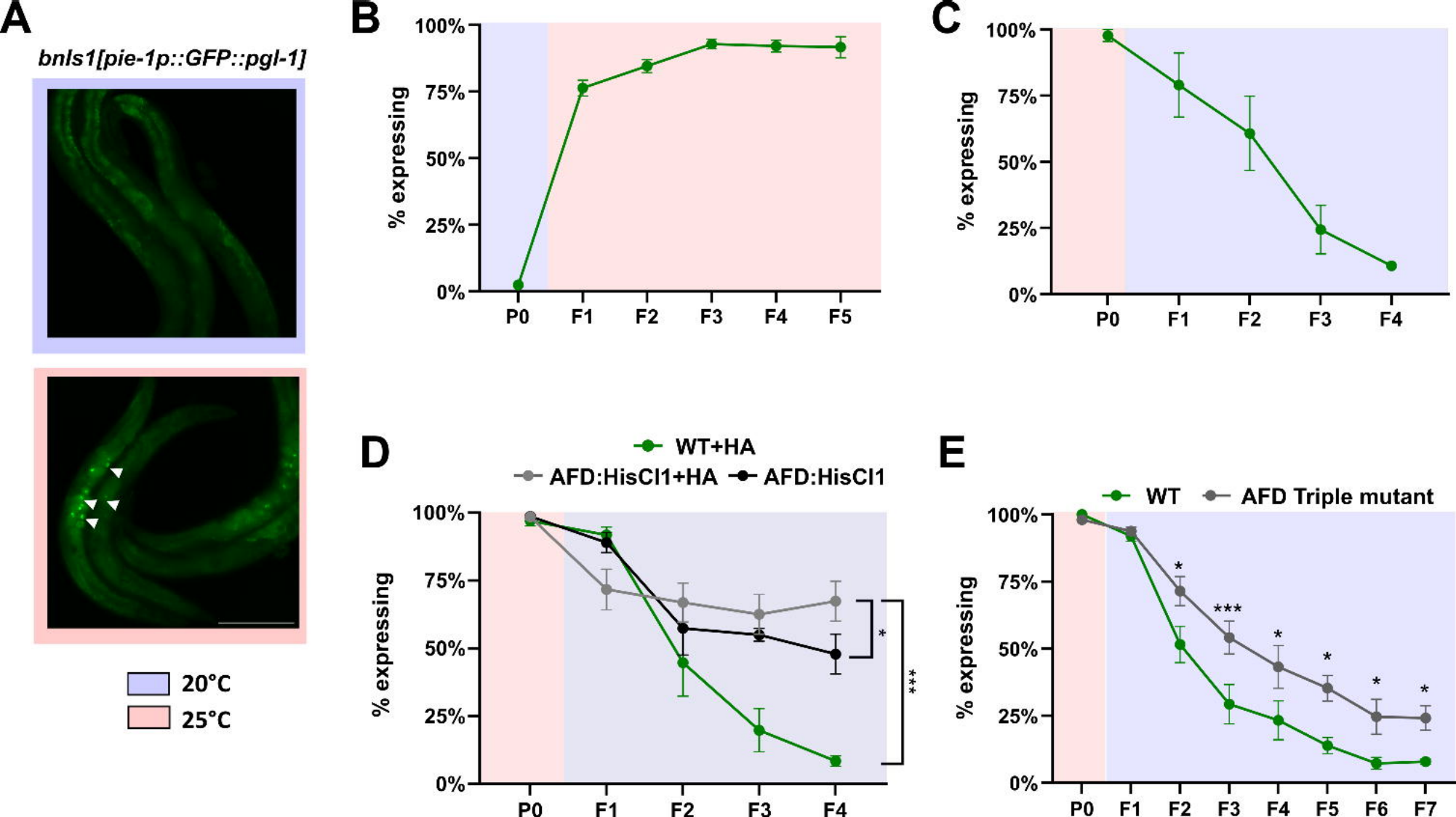
A
bnls1[pie-1p::GFP::pgl-1]
20°C
25°C
B
% expressing
100%
75%
50%
25%
0%
P0
F1
F2
F3
F4
F5
C
% expressing
100%
75%
50%
25%
0%
P0
F1
F2
F3
F4
D
WT+HA
AFD:HisCl1+HA
AFD:HisCl1
% expressing
100%
75%
50%
25%
0%
*
***
P0
F1
F2
F3
F4
E
WT
AFD Triple mutant
% expressing
100%
75%
50%
25%
0%
*
***
*
*
*
*
P0
F1
F2
F3
F4
F5
F6
F7

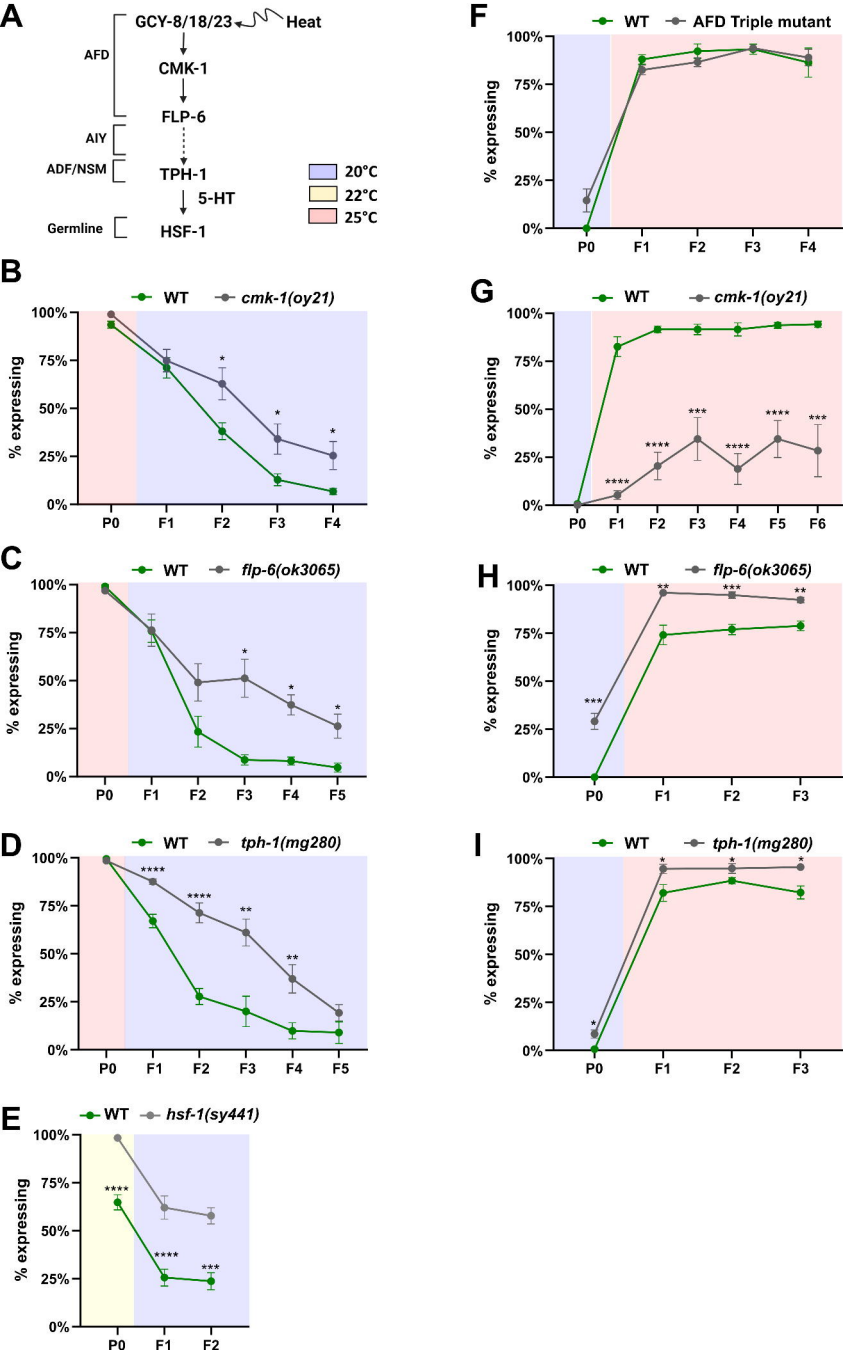
A
GCY-8/18/23
Heat
AFD
CMK-1
FLP-6
AIY
ADF/NSM
TPH-1
5-HT
Germline
HSF-1
20°C
22°C
25°C
B
WT
cmk-1(oy21)
% expressing
P0 F1 F2 F3 F4
C
WT
flp-6(ok3065)
P0 F1 F2 F3 F4 F5
D
WT
tph-1(mg280)
P0 F1 F2 F3 F4 F5
E
WT
hsf-1(sy441)
P0 F1 F2
F
WT
AFD Triple mutant
P0 F1 F2 F3 F4
G
WT
cmk-1(oy21)
P0 F1 F2 F3 F4 F5 F6
H
WT
flp-6(ok3065)
P0 F1 F2 F3
I
WT
tph-1(mg280)
P0 F1 F2 F3

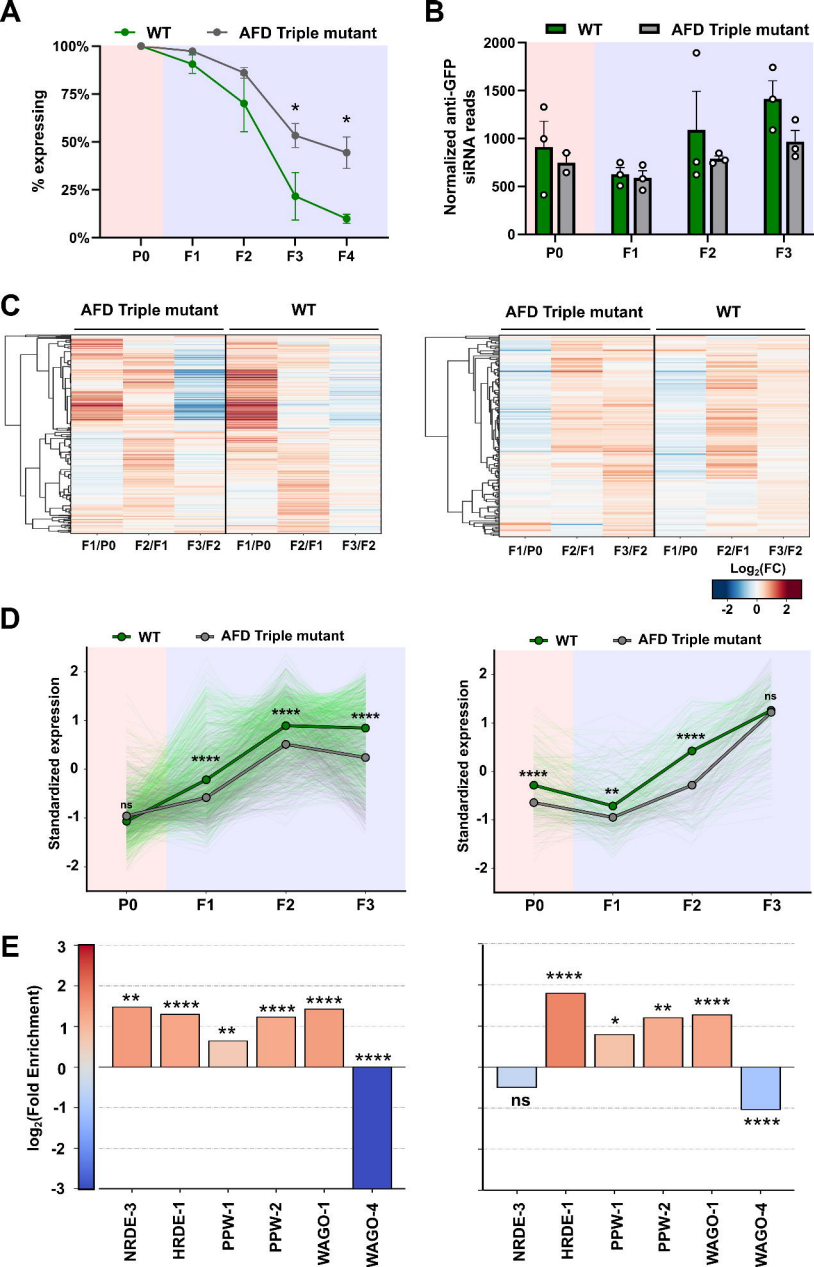
A
WT
AFD Triple mutant
100%
75%
50%
25%
0%
% expressing
P0
F1
F2
F3
F4
*
*
B
WT
AFD Triple mutant
2000
1500
1000
500
0
Normalized anti-GFP siRNA reads
P0
F1
F2
F3
C
AFD Triple mutant
WT
AFD Triple mutant
WT
F1/P0
F2/F1
F3/F2
F1/P0
F2/F1
F3/F2
F1/P0
F2/F1
F3/F2
F1/P0
F2/F1
F3/F2
Log2(FC)
-2
0
2
D
WT
AFD Triple mutant
Standardized expression
2
1
0
-1
-2
ns
****
****
****
P0
F1
F2
F3
WT
AFD Triple mutant
Standardized expression
****
**
****
ns
P0
F1
F2
F3
E
log2(Fold Enrichment)
3
2
1
0
-1
-2
-3
**
****
**
****
****
****
NRDE-3
HRDE-1
PPW-1
PPW-2
WAGO-1
WAGO-4
ns
****
*
**
****
****
NRDE-3
HRDE-1
PPW-1
PPW-2
WAGO-1
WAGO-4

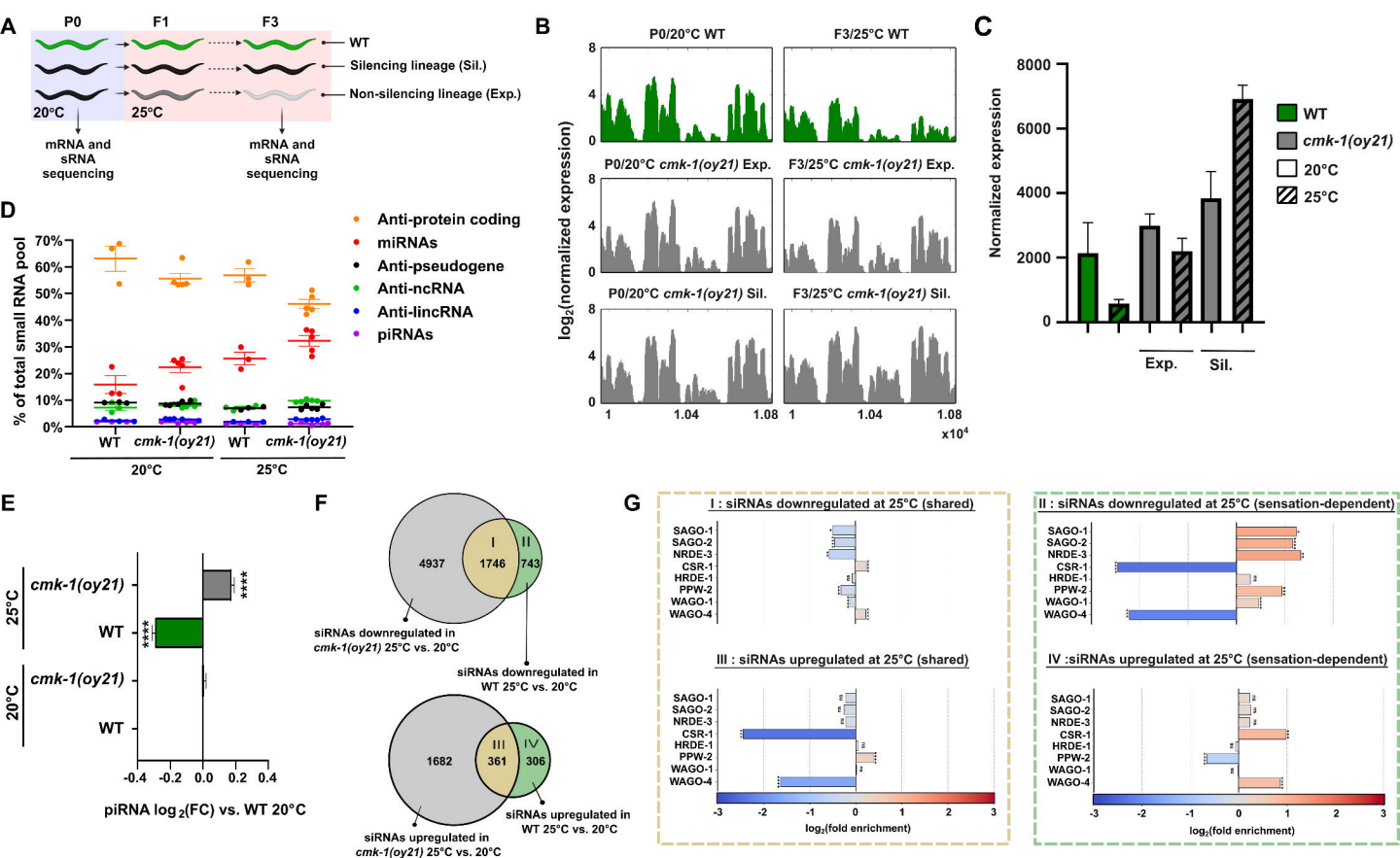
A
P0
F1
F3
WT
Silencing lineage (Sil.)
Non-silencing lineage (Exp.)
20°C
25°C
mRNA and sRNA sequencing
mRNA and sRNA sequencing
B
P0/20°C WT
F3/25°C WT
P0/20°C cmk-1(oy21) Exp.
F3/25°C cmk-1(oy21) Exp.
P0/20°C cmk-1(oy21) Sil.
F3/25°C cmk-1(oy21) Sil.
log2(normalized expression)
x10^4
C
Normalized expression
WT
cmk-1(oy21)
20°C
25°C
Exp.
Sil.
D
% of total small RNA pool
Anti-protein coding
miRNAs
Anti-pseudogene
Anti-ncRNA
Anti-lincRNA
piRNAs
WT
cmk-1(oy21)
20°C
25°C
E
cmk-1(oy21)
WT
piRNA log2(FC) vs. WT 20°C
F
4937
1746
743
siRNAs downregulated in cmk-1(oy21) 25°C vs. 20°C
siRNAs downregulated in WT 25°C vs. 20°C
1682
361
306
siRNAs upregulated in cmk-1(oy21) 25°C vs. 20°C
siRNAs upregulated in WT 25°C vs. 20°C
G
I : siRNAs downregulated at 25°C (shared)
II : siRNAs downregulated at 25°C (sensation-dependent)
III : siRNAs upregulated at 25°C (shared)
IV :siRNAs upregulated at 25°C (sensation-dependent)
SAGO-1
SAGO-2
NRDE-3
CSR-1
HRDE-1
PPW-2
WAGO-1
WAGO-4
log2(fold enrichment)

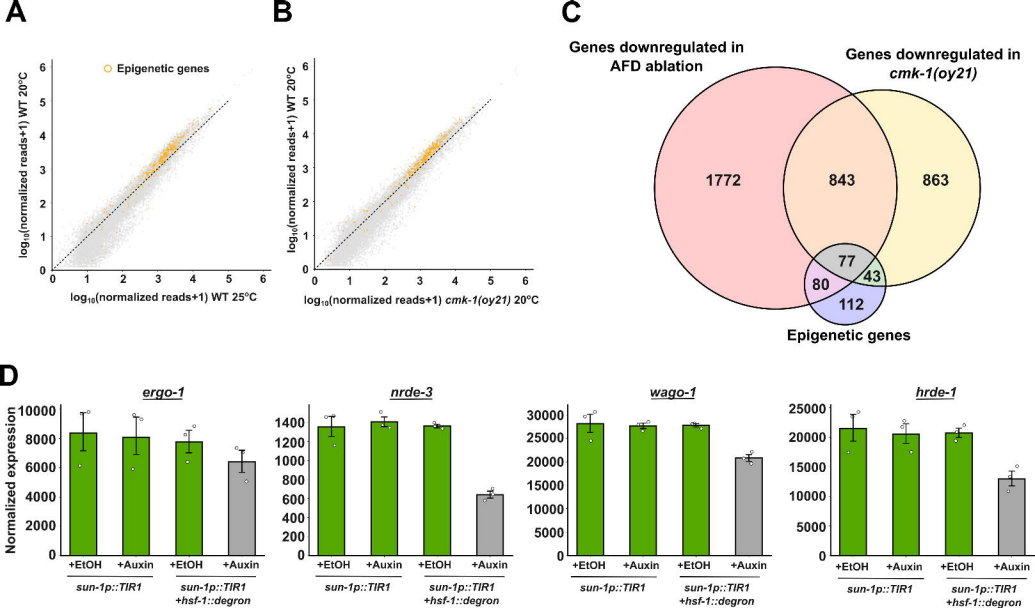
A
B
C
D
Epigenetic genes
log10(normalized reads+1) WT 20°C
log10(normalized reads+1) WT 25°C
log10(normalized reads+1) cmk-1(oy21) 20°C
Genes downregulated in AFD ablation
Genes downregulated in cmk-1(oy21)
Epigenetic genes
1772
843
863
77
43
80
112
Normalized expression
ergo-1
nrde-3
wago-1
hrde-1
+EtOH
+Auxin
sun-1p::TIR1
sun-1p::TIR1 +hsf-1::degron

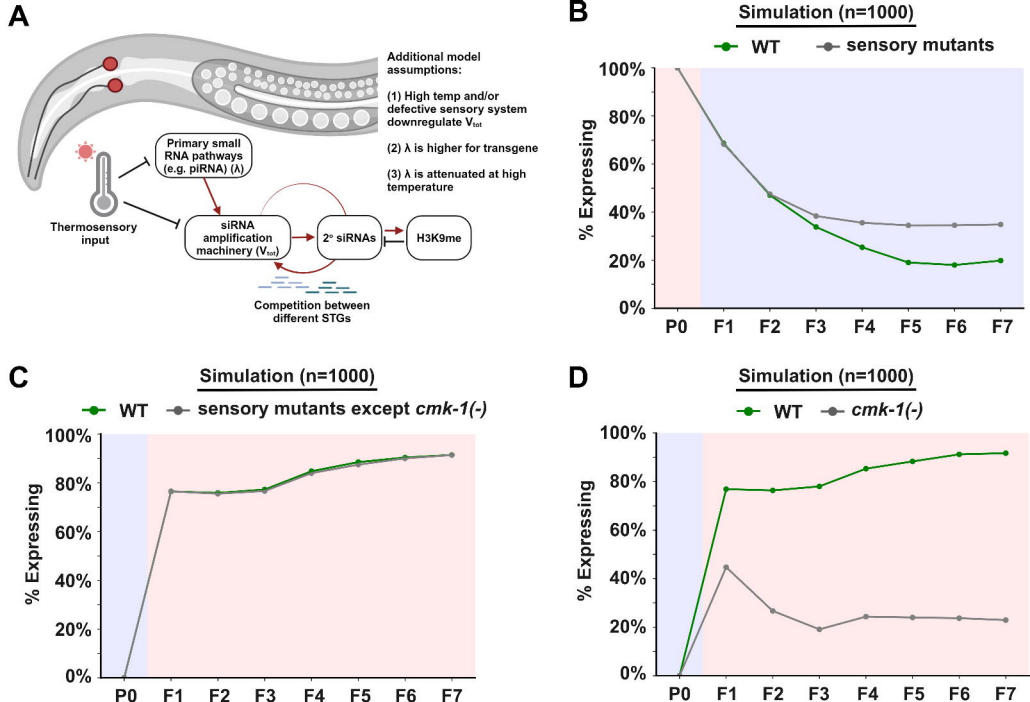
A
Additional model assumptions:
(1) High temp and/or defective sensory system downregulate V_{tot}
(2) λ is higher for transgene
(3) λ is attenuated at high temperature
Primary small RNA pathways (e.g. piRNA) (λ)
Thermosensory input
siRNA amplification machinery (V_{tot})
2° siRNAs
H3K9me
Competition between different STGs
B
Simulation (n=1000)
WT
sensory mutants
% Expressing
100%
80%
60%
40%
20%
0%
P0 F1 F2 F3 F4 F5 F6 F7
C
Simulation (n=1000)
WT
sensory mutants except cmk-1(-)
% Expressing
100%
80%
60%
40%
20%
0%
P0 F1 F2 F3 F4 F5 F6 F7
D
Simulation (n=1000)
WT
cmk-1(-)
% Expressing
100%
80%
60%
40%
20%
0%
P0 F1 F2 F3 F4 F5 F6 F7

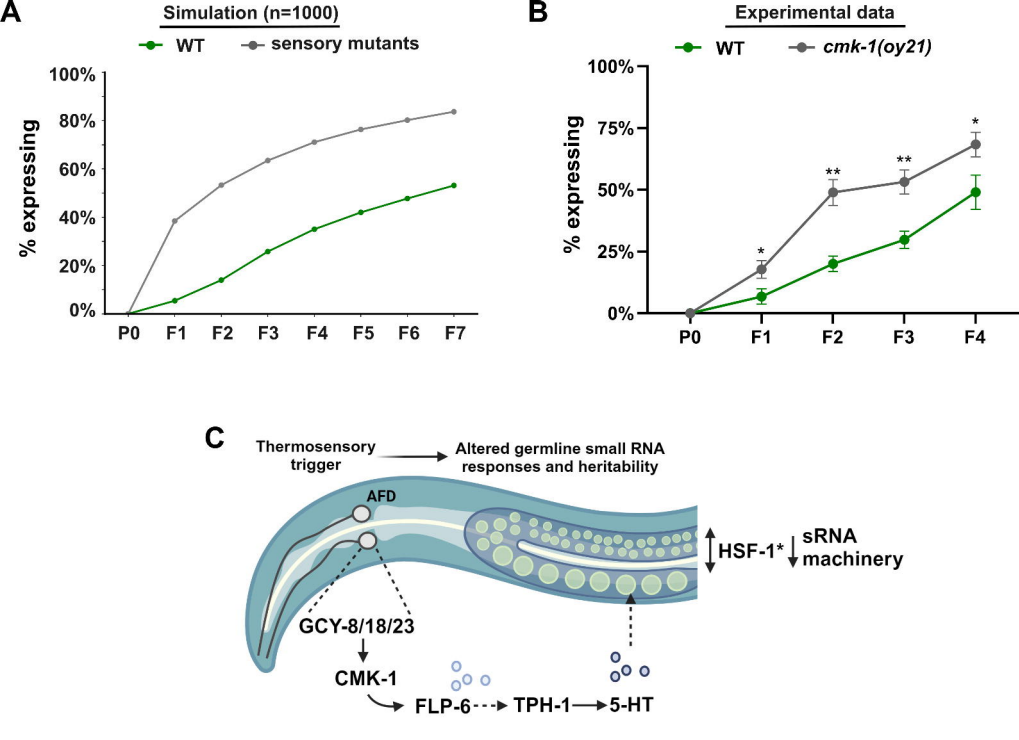
A
Simulation (n=1000)
WT
sensory mutants
% expressing
100%
80%
60%
40%
20%
0%
P0
F1
F2
F3
F4
F5
F6
F7
B
Experimental data
WT
cmk-1(oy21)
% expressing
100%
75%
50%
25%
0%
*
**
**
*
P0
F1
F2
F3
F4
C
Thermosensory trigger
Altered germline small RNA responses and heritability
AFD
HSF-1*
sRNA machinery
GCY-8/18/23
CMK-1
FLP-6
TPH-1
5-HT

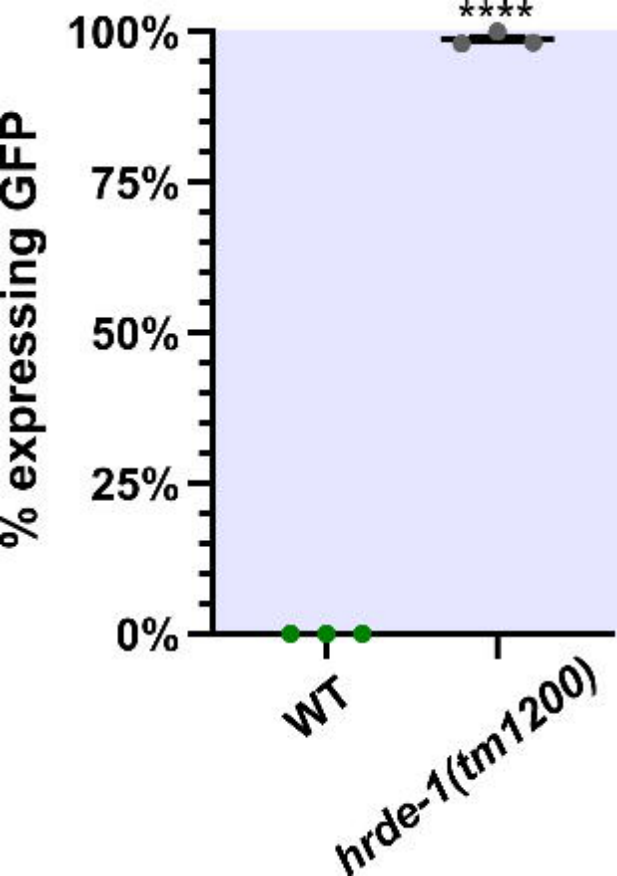
****
100%
75%
50%
25%
0%
% expressing GFP
WT
hrde-1(tm1200)

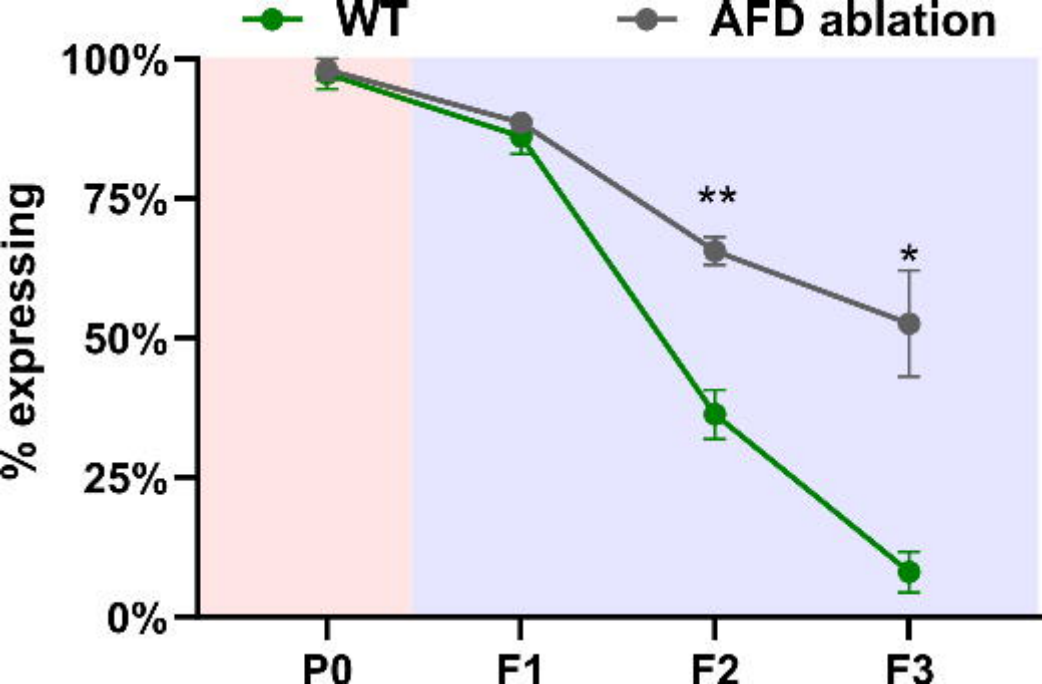
WT
AFD ablation
100%
75%
50%
25%
0%
% expressing
**
*
P0
F1
F2
F3

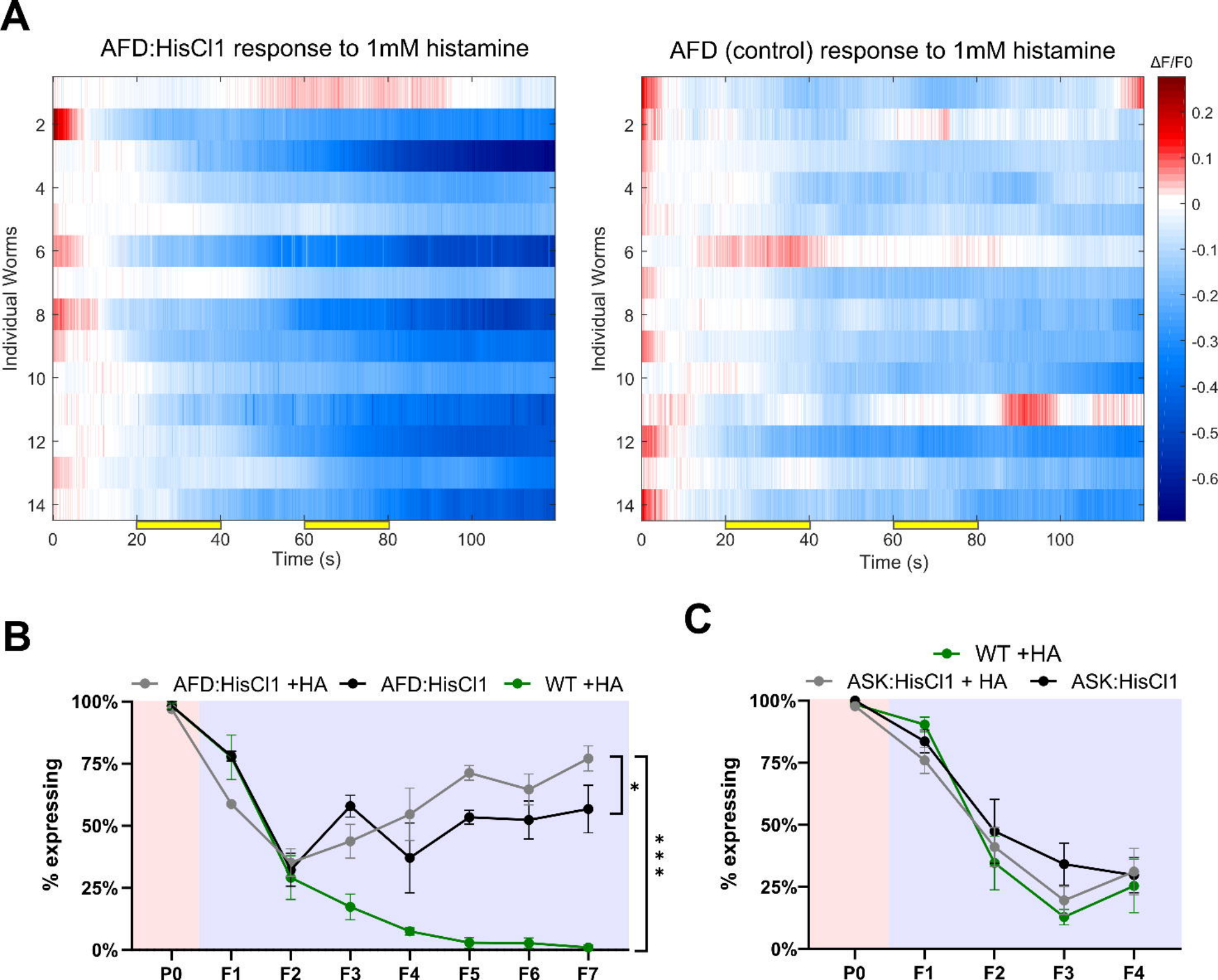
A
AFD:HisCl1 response to 1mM histamine
AFD (control) response to 1mM histamine
ΔF/F0
0.2
0.1
0
-0.1
-0.2
-0.3
-0.4
-0.5
-0.6
Individual Worms
2
4
6
8
10
12
14
0
20
40
60
80
100
Time (s)
B
AFD:HisCl1 +HA
AFD:HisCl1
WT +HA
% expressing
100%
75%
50%
25%
0%
P0
F1
F2
F3
F4
F5
F6
F7
*
***
C
WT +HA
ASK:HisCl1 + HA
ASK:HisCl1
% expressing
100%
75%
50%
25%
0%
P0
F1
F2
F3
F4

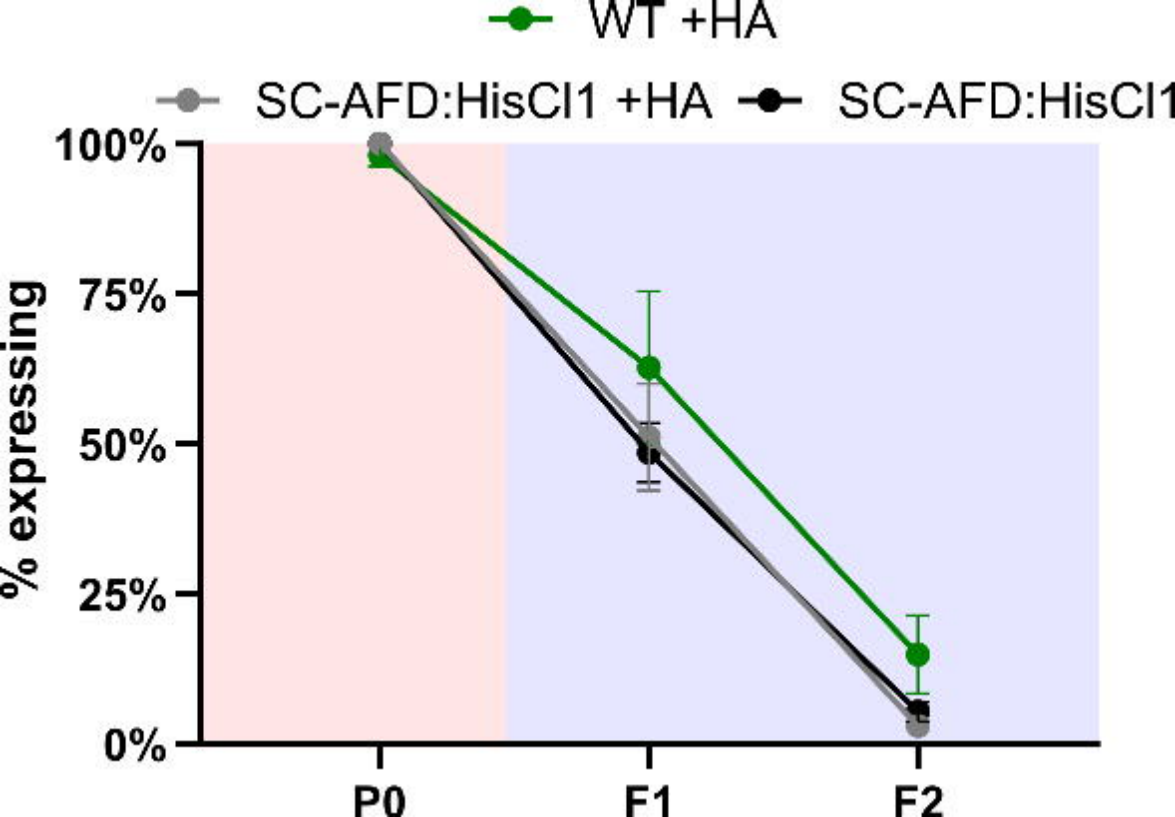
WT +HA
SC-AFD:HisCl1 +HA
SC-AFD:HisCl1
100%
75%
50%
25%
0%
% expressing
P0
F1
F2

A

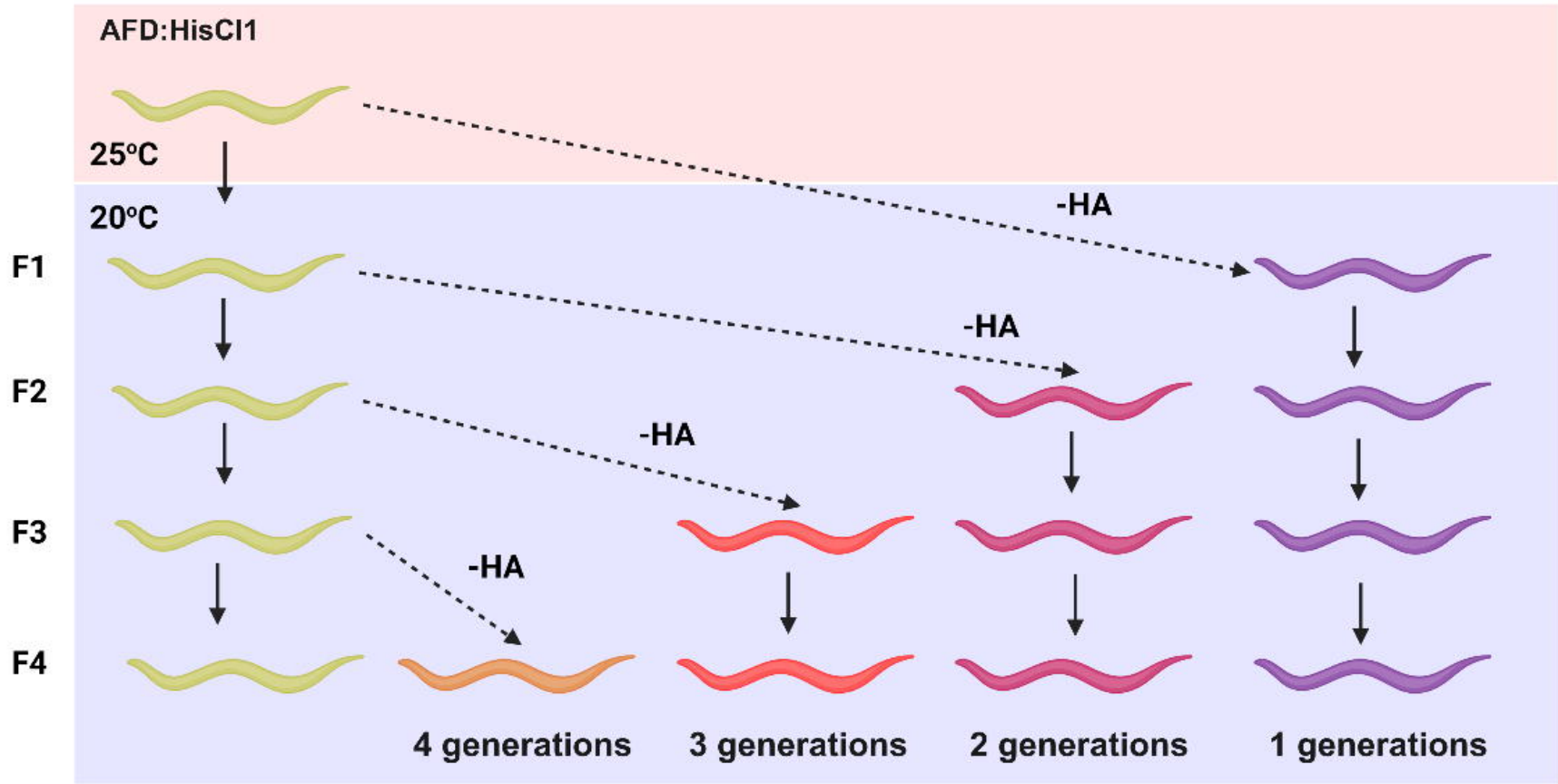
AFD:HisCl1
25°C
20°C
F1
F2
F3
F4
-HA
-HA
-HA
-HA
4 generations
3 generations
2 generations
1 generations

B

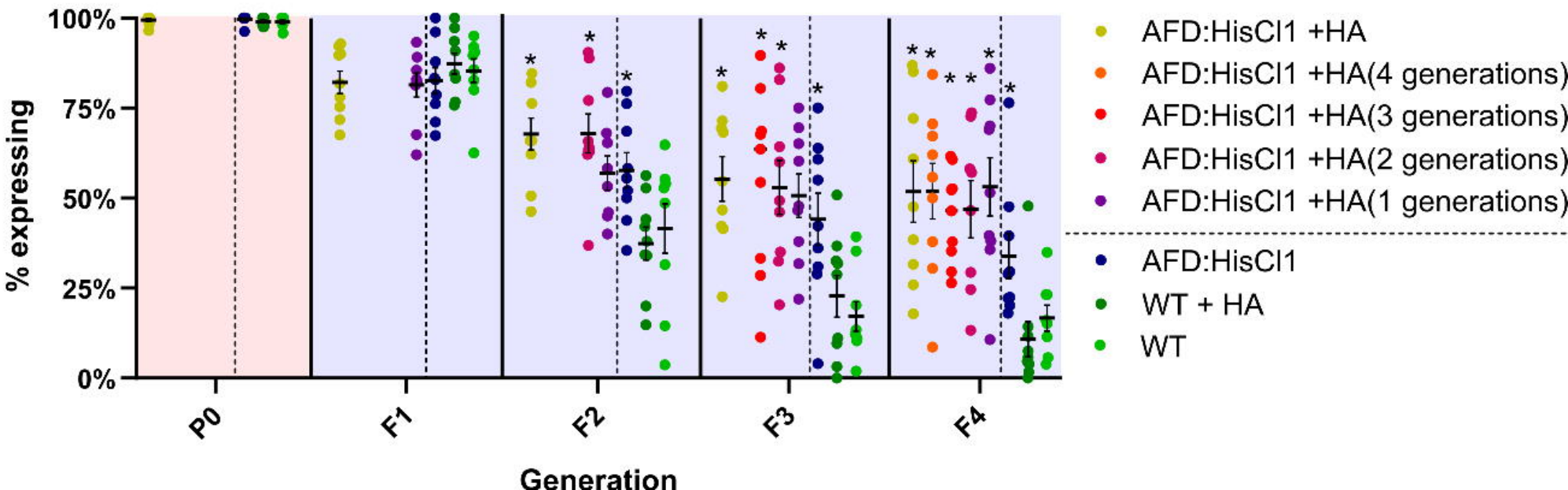
100%
75%
50%
25%
0%
% expressing
P0
F1
F2
F3
F4
Generation
AFD:HisCl1 +HA
AFD:HisCl1 +HA(4 generations)
AFD:HisCl1 +HA(3 generations)
AFD:HisCl1 +HA(2 generations)
AFD:HisCl1 +HA(1 generations)
AFD:HisCl1
WT + HA
WT

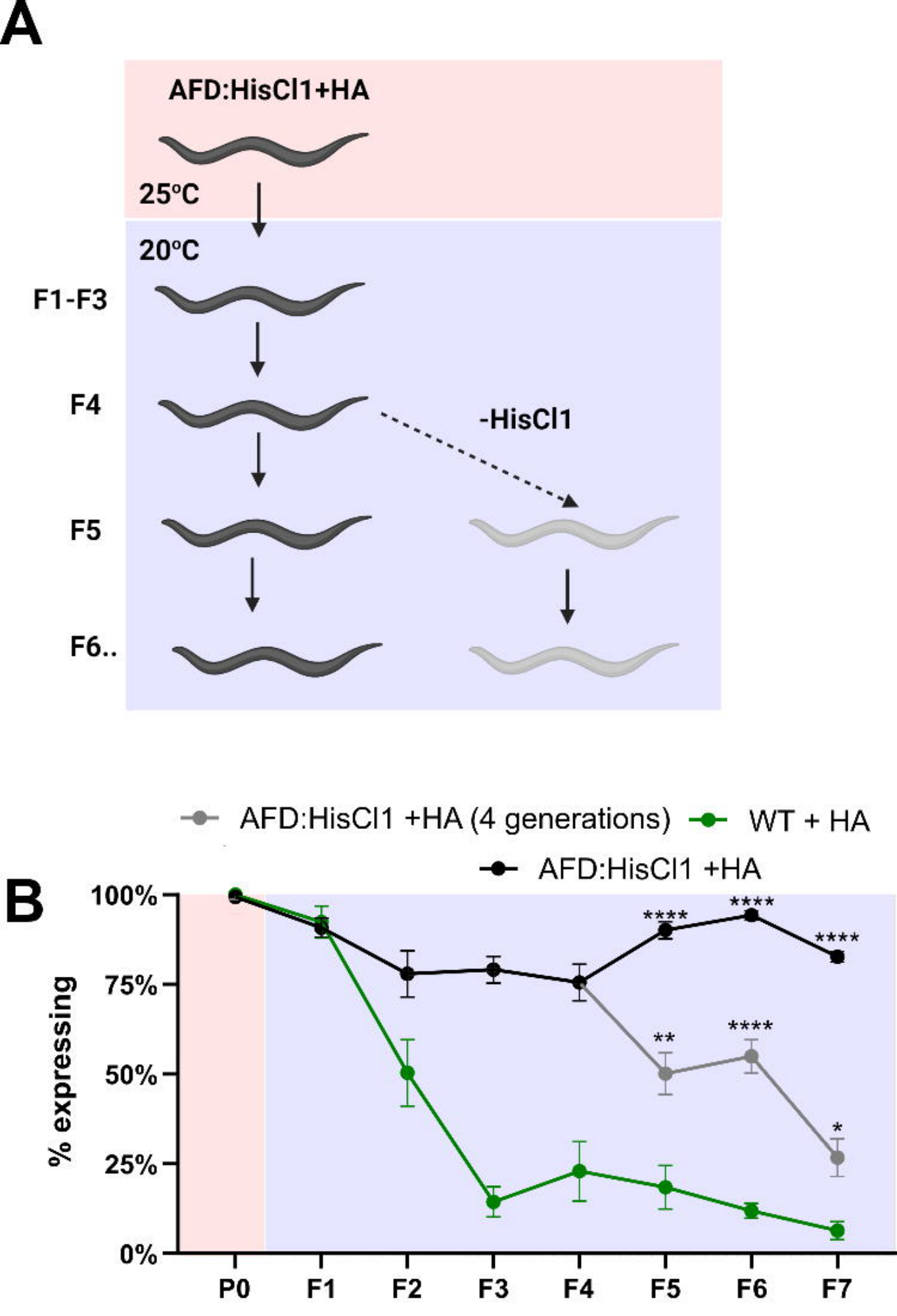
A
AFD:HisCl1+HA
25°C
20°C
F1-F3
F4
-HisCl1
F5
F6..
B
AFD:HisCl1 +HA (4 generations)
WT + HA
AFD:HisCl1 +HA
% expressing
100%
75%
50%
25%
0%
P0
F1
F2
F3
F4
F5
F6
F7
****
****
****
**
****
*

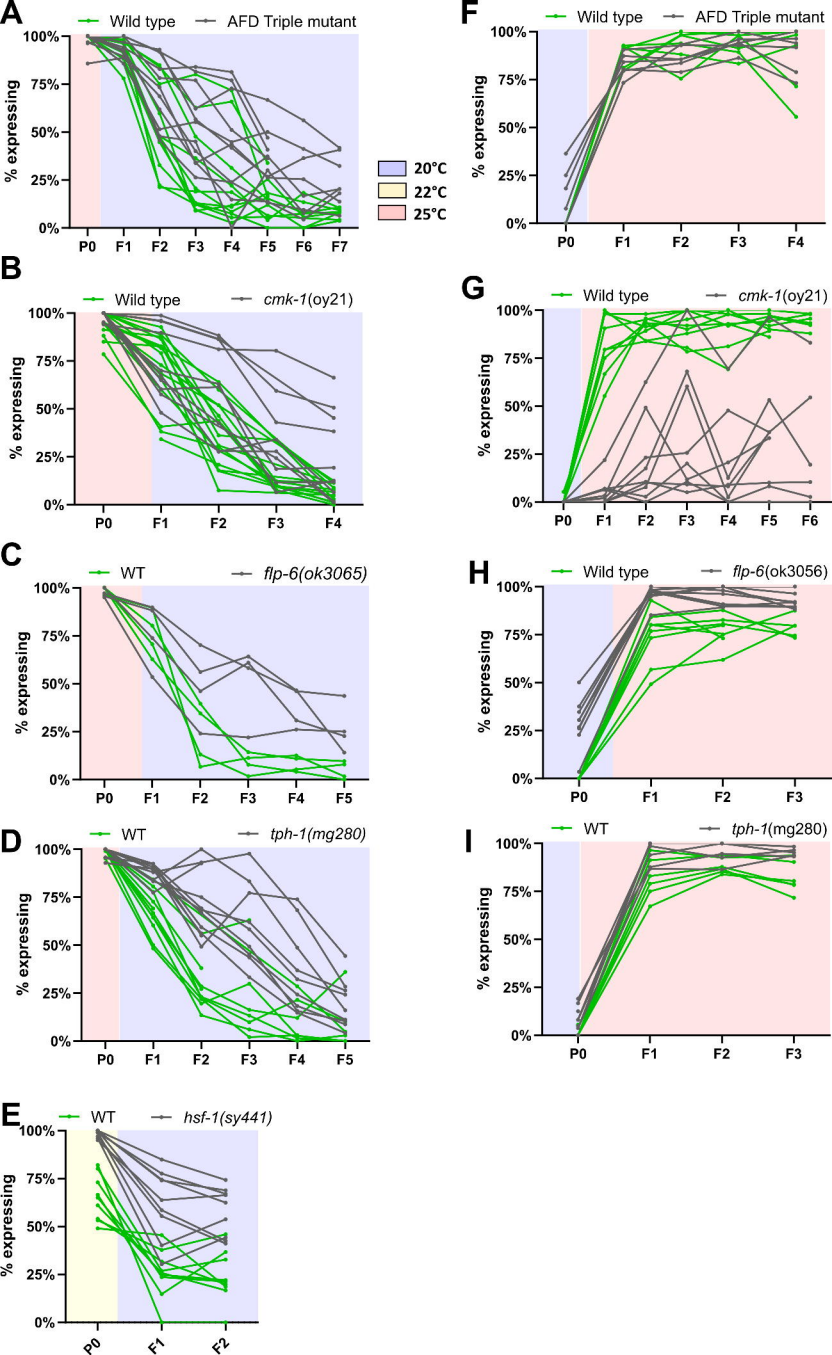
A
Wild type
AFD Triple mutant
% expressing
100%
75%
50%
25%
0%
P0 F1 F2 F3 F4 F5 F6 F7
20°C
22°C
25°C
B
Wild type
cmk-1(oy21)
% expressing
P0 F1 F2 F3 F4
C
WT
flp-6(ok3065)
% expressing
P0 F1 F2 F3 F4 F5
D
WT
tph-1(mg280)
% expressing
P0 F1 F2 F3 F4 F5
E
WT
hsf-1(sy441)
% expressing
P0 F1 F2
F
Wild type
AFD Triple mutant
% expressing
P0 F1 F2 F3 F4
G
Wild type
cmk-1(oy21)
% expressing
P0 F1 F2 F3 F4 F5 F6
H
Wild type
flp-6(ok3056)
% expressing
P0 F1 F2 F3
I
WT
tph-1(mg280)
% expressing
P0 F1 F2 F3

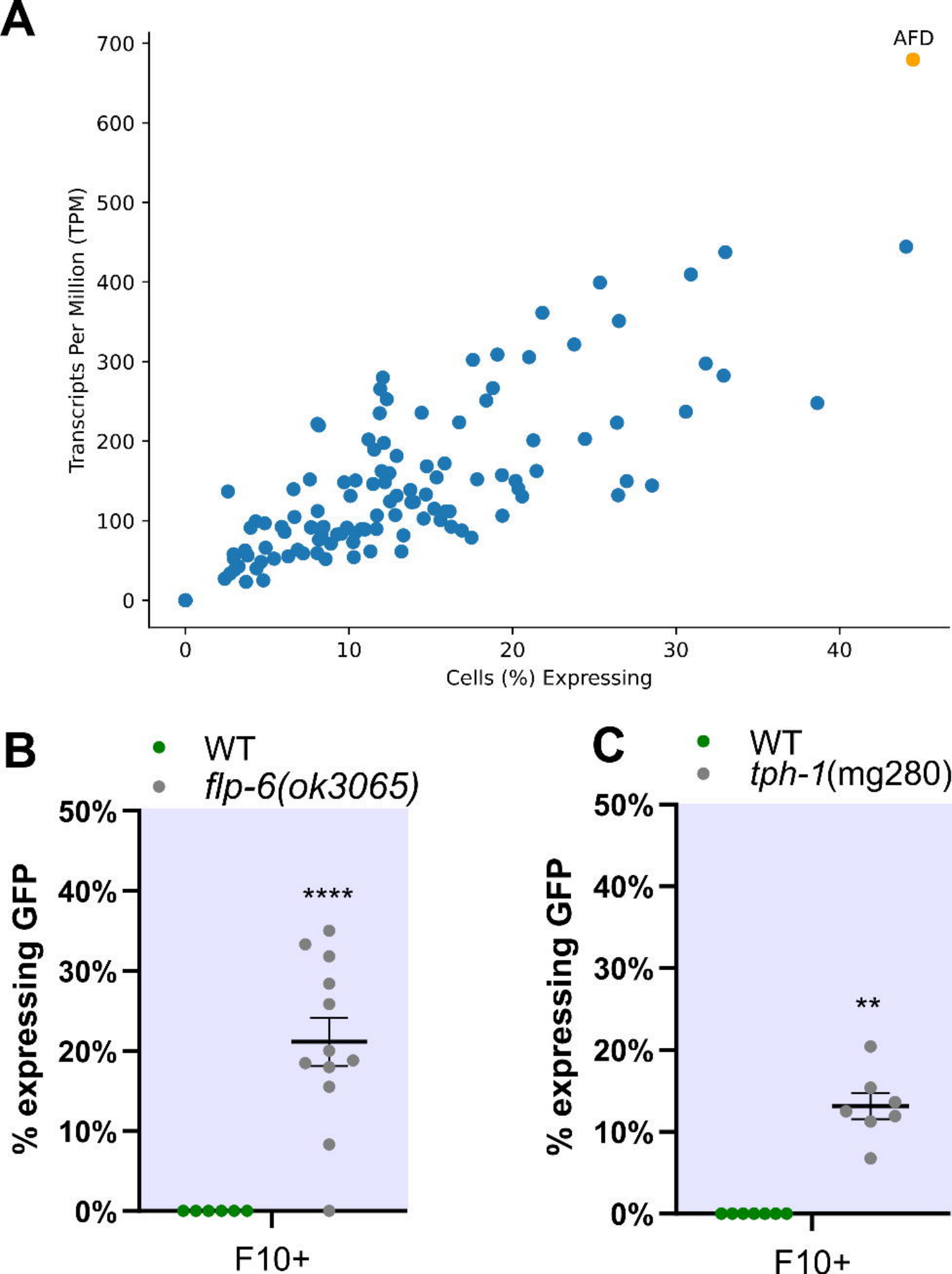
A
AFD
Transcripts Per Million (TPM)
Cells (%) Expressing
B
WT
flp-6(ok3065)
% expressing GFP
****
F10+
C
WT
tph-1(mg280)
% expressing GFP
**
F10+

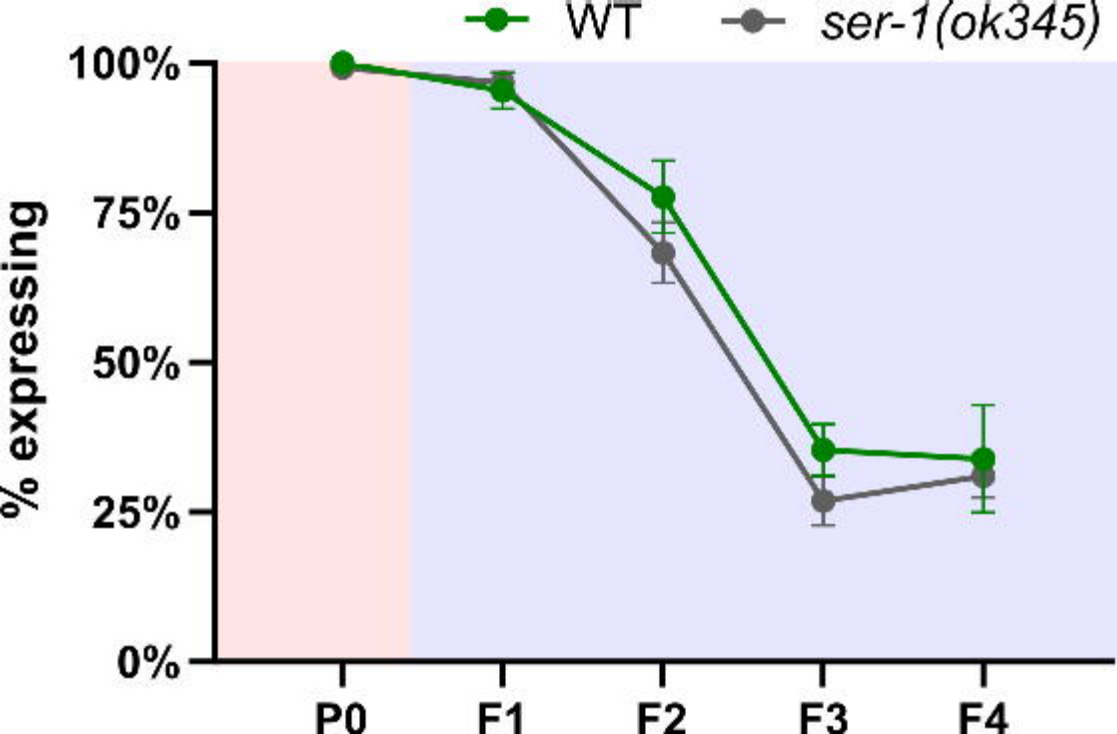
WT
ser-1(ok345)
100%
75%
50%
25%
0%
% expressing
P0
F1
F2
F3
F4

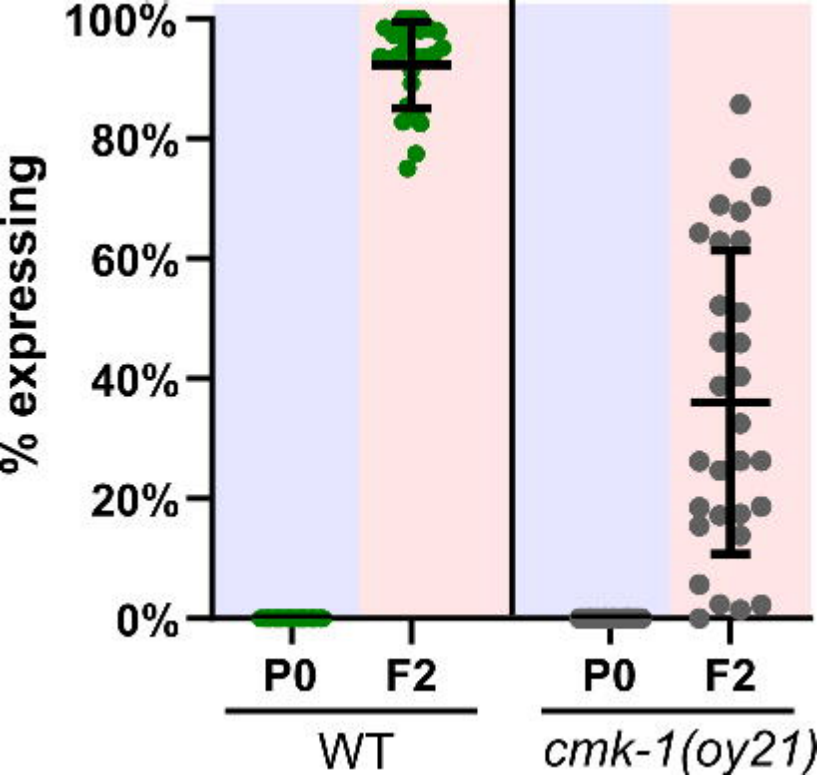
100%
80%
60%
40%
20%
0%
% expressing
P0
F2
P0
F2
WT
cmk-1(oy21)

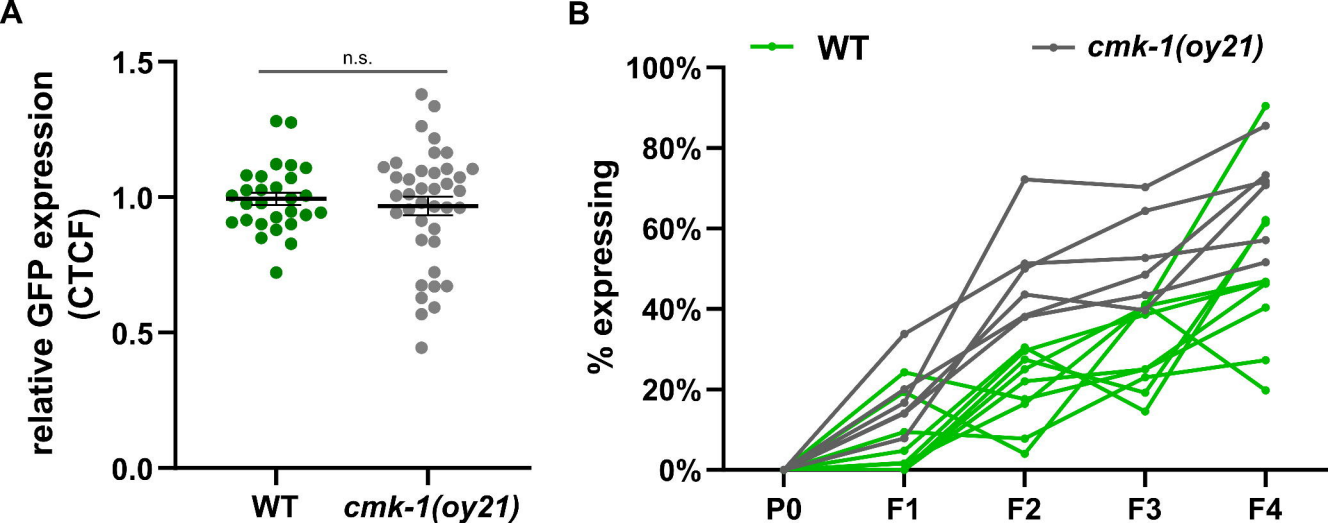
A
relative GFP expression (CTCF)
1.5
1.0
0.5
0.0
n.s.
WT
cmk-1(oy21)
B
WT
cmk-1(oy21)
% expressing
100%
80%
60%
40%
20%
0%
P0
F1
F2
F3
F4